

Dimensionless machine learning: Imposing exact units equivariance

Soledad Villar

SOLEDAD.VILLAR@JHU.EDU

Department of Applied Mathematics and Statistics, Johns Hopkins University

Mathematical Institute for Data Science, Johns Hopkins University

Weichi Yao

WEICHI.YAO@NYU.EDU

Department of Technology, Operations and Statistics, New York University

David W. Hogg

DAVID.HOGG@NYU.EDU

Center for Cosmology and Particle Physics, Department of Physics, New York University

Max-Planck-Institut für Astronomie

Flatiron Institute, a Division of the Simons Foundation

Ben Blum-Smith

BEN@CIMS.NYU.EDU

Center for Data Science, New York University

Bianca Dumitrascu

BMD39@CAM.AC.UK

Department of Computer Science and Technology, Cambridge University

Abstract

Units equivariance is the exact symmetry that follows from the requirement that relationships among measured quantities of physics relevance must obey self-consistent dimensional scalings. Here, we employ dimensional analysis and ideas from equivariant machine learning to provide a two stage learning procedure for units-equivariant machine learning. For a given learning task, we first construct a dimensionless version of its inputs using classic results from dimensional analysis, and then perform inference in the dimensionless space. Our approach can be used to impose units equivariance across a broad range of machine learning methods which are equivariant to rotations and other groups. We discuss the in-sample and out-of-sample prediction accuracy gains one can obtain in contexts like symbolic regression and emulation, where symmetry is important. We illustrate our approach with simple numerical examples involving dynamical systems in physics and ecology.

1. Introduction

In recent years, there has been enormous progress in developing machine learning methods which incorporate exact symmetries. Some of these methods involve group convolutions (Cohen and Welling, 2016, 2017; Wang et al., 2020a), irreducible representations of groups (Fuchs et al., 2020; Kondor, 2018; Thomas et al., 2018; Weiler et al., 2018; Cohen et al., 2018; Weiler and Cesa, 2019) or constraints (Finzi et al., 2021), while others involve the construction of explicitly invariant features (Gripaios et al., 2021; Haddadin, 2021; Villar et al., 2021; Yao et al., 2021). Indeed, the revolutionary performance of convolutional neural networks (LeCun et al., 1989) was enabled by the imposition of a local translational symmetry at the bottom layer of the networks. When a learning problem obeys an exact symmetry, we have the strong intuition that imposing that symmetry must improve learning and generalization, and there is now theoretical work supporting this intuition (Elesedy and Zaidi, 2021; Bietti

et al., 2021; Mei et al., 2021). Much of this work has been situated in the physics domain (Yu et al., 2021; Kashinath et al., 2021), because physical laws exactly obey a panoply of symmetries.

One of the symmetries of physics—and indeed all of the sciences—is the symmetry underlying dimensional analysis. Quantities that are added or subtracted must have identical units. And if the units system of the inputs to a function is changed, the units of the output must change accordingly. This symmetry—which we will call “units equivariance” has many implications. One is that it is possible to derive scalings and dependencies of outputs on inputs from the units directly. For example, if a problem involves only a length L , an acceleration g , and a mass m , and the problem is to learn or predict a time t , it is possible from units alone to see that $t \propto \sqrt{L/g}$. Another implication is that most nonlinear functions (such as transcendental functions or even ReLU functions; Agarap 2018) can only be applied to dimensionless quantities. If a quantity x is dimensional, almost any polynomial expression of x is inconsistent with the principle that quantities to be added or subtracted must have identical units; thus most non-linear functions must be a function only of dimensionless inputs. These symmetries are strict and exact, and not just in physics: In chemistry, ecology, and economics, for examples, the inputs and the outputs of functional relationships have non-trivial units, and the results must be equivariant to the choice of units system.

The laws of the natural sciences obey strong symmetries. Observed data sets do not always show these symmetries as clearly, because investigator choices and the location and state of observing or measuring hardware can break those symmetries. For example, the Universe is isotropic and homogeneous, but our observations of the Universe are anisotropic and inhomogeneous, because we observe different parts of the Universe and in different directions with different fidelity. However, the fundamental theories are exactly symmetric. This suggests that the imposition of exact symmetries might be most important in contexts in which machine learning methods are being used to emulate theoretical simulations. In particular, when attempting to find symbolic expressions (for example, Cranmer et al. 2020; Udrescu and Tegmark 2020) matching data from unknown quantities of practical physical interest, symmetries are not only unavoidable, they also enable learning by constraining the large, combinatorial, otherwise unidentifiable space of generic functions (Udrescu and Tegmark, 2020). These considerations apply to all symmetries, including the units equivariance we establish and exploit here.

The work presented here is in the context of group equivariant machine learning (Cohen and Welling, 2016; Maron et al., 2018; Kondor, 2018) and builds on previous work on machine learning for physics, in which it has been shown that group-invariant scalars are the only inputs needed by a machine learning method, if the goal is to learn group-equivariant functions of geometric objects (such as scalars, vectors, and tensors; Villar et al. 2021; Yao et al. 2021). With what is developed here, we can make these scalars *dimensionless* before they are used as inputs, and then scale the dimensions or units back in before the final outputs are delivered (or before cost functions are evaluated). In all these projects, the fundamental philosophy is to transform the features into invariant forms before they are used to train the machine learning method, and then to un-transform label predictions at the output or at test time. These approaches to symmetry-respecting machine learning are simple to implement and perform extremely well (Yao et al., 2021).

Our contributions:

- We define a *units equivariance* and incorporate it into machine learning models using ideas from classical dimensional analysis.
- We show that exact units equivariance is easy to impose on many kinds of learning tasks, by constructing a dimensionless version of the learning task, performing the dimensionless task, and then scaling back in the proper dimensions (and units) at the end (perhaps prior to evaluating the cost function). Dimensionless quantities are invariants with respect to changes of units and can be computed using discrete linear algebra algorithms. In this sense, the approach we advocate here is related to approaches based on group invariants to impose exact group equivariances (Villar et al., 2021).
- We briefly discuss how imposing units equivariance allows for out-of-distribution generalization, and in the case of linear regressions, decreases the risk of the estimators (Section 5).
- We discuss extensions of theoretical results on generalization bounds for regression problems under symmetries generated by compact groups (Elesedy and Zaidi, 2021), to the group of scalings (which is not compact but reductive).
- We demonstrate with a few simple numerical regression problems that the reduction of model capacity (at fixed complexity) delivered by the units equivariance leads to improvements in generalization. In this context, we discuss symbolic regression and emulator related tasks. We also discuss limitations of our approach in the context of unknown dimensional constants.

Related work: Dimensional analysis is a classical theory with applications in engineering and science (Barenblatt 1996 is a comprehensive textbook in the subject). These ideas have been connected to machine learning previously (Rudolph et al., 1998; Frisone and Misiti, 2019; Bakarji et al., 2022). The key theoretical result in dimensional analysis is the Buckingham Pi Theorem (Buckingham, 1914), which says that a function is units equivariant if and only if it is a function of a set of dimensionless scalars, obtained as products of integer powers of the input features, with appropriate scaling. Integer linear algebra algorithms allow us to find a generating set of dimensionless features (Hubert and Labahn, 2012). In this work we use these dimensionless features to produce units-equivariant machine-learning methods.

Machine-learning methods based on neural networks have shown to be extremely successful, significantly advancing the state of the art in many scientific tasks. However, the design of the neural networks is key for their success. Many of the design choices are based on exact or approximate symmetries satisfied by the data or the problem. Recent work has incorporated group invariances and equivariances to the design of the architectures. The most common example is graph neural networks, where learned functions are equivariant with respect to a certain action by permutations which change the order in which the nodes appear in the adjacency matrix (Gilmer et al., 2017; Duvenaud et al., 2015; Chen et al., 2019a; Gama et al., 2020). This has been extended to general groups and actions, leading to

the field of equivariant machine learning, which restricts the class of neural neural networks to only represent functions that are invariant or equivariant with respect to a certain group action (Maron et al., 2018). This requires to be able to parameterize the space of equivariant functions, which is not always computationally easy (Xu et al., 2018; Morris et al., 2019; Chen et al., 2019b, 2020b). Methods include group convolutions (Cohen and Welling, 2016, 2017; Wang et al., 2020c), irreducible representations (Fuchs et al., 2020; Kondor, 2018; Thomas et al., 2018; Weiler et al., 2018; Cohen et al., 2018; Weiler and Cesa, 2019), constraints (Finzi et al., 2021), and classical invariant theory to design invariant features (Gripaios et al., 2021; Haddadin, 2021; Villar et al., 2021). Applications of equivariant machine learning span from molecular dynamics, to turbulence, to climate and traffic prediction (Batzner et al., 2021; Wang et al., 2020b; Bakarji et al., 2022; Kashinath et al., 2021; Jin et al., 2020), to name a few directions.

The reason why one may want to impose symmetries is intuitive. Many systems, in particular physical systems, are constrained by the laws of physics, which satisfy exact symmetries. A related approach is provided by the physics-informed machine learning literature (Karniadakis et al., 2021), where expertise from classical numerical analysis and scientific computing are incorporated into machine learning pipelines. For instance, machine learning methods that make use of highly accurate numerical integrators.

The imposition of symmetries can improve inductive bias when the symmetries encode correct domain knowledge. One may expect it to reduce the sample complexity and generalization error. A recent line of work develops mathematical theory to quantify the benefits of imposing symmetries and group equivariance in regression problems. The work of Elesedy and Zaidi (2021) provides a computation of the excess risk in the context of linear regression, then extended to kernel regressions in Elesedy (2021). The works of Bietti et al. (2021) and Mei et al. (2021) focus on quantifying the sample complexity gain for regressions with (finite) group-invariant kernels. The work by Brugiapaglia et al. (2021) show that certain symmetries have to be imposed or otherwise many learning algorithms are not able to learn correctly.

Further, numerous studies have explored data augmentation as an approach to empirically encourage invariance and symmetries. Data augmentation techniques aim to expand (or augment) training data sets with properly transformed data points that retain crucial properties of the original training data. Data augmentation has a long history (Baird, 1992; Van Dyk and Meng, 2001) with many techniques shown to yield empirical improvements in a variety of tasks (Wong et al., 2016; Cubuk et al., 2018, 2020). Recently, theoretical treatments have also been proposed to augment the favorable empirical performance (Dao et al., 2019; Chen et al., 2020a; Shen et al., 2022). A recent group-theoretic treatment (Chen et al., 2020a) showed that data augmentation can lead to variance reduction properties in the context of empirical risk minimization. In another study, data augmentation is characterized as a way to alter the relative importances of features and is shown to be less likely to overfit to noise (Shen et al., 2022).

Here we will end up assuming that the dimensions and units of all regression inputs are known, complete, and self consistent. However, a different direction would be to look at how dimensional relationships or other symmetries are *discovered*. This is the setting for Constantine et al. (2017), and Evangelou et al. (2021). This idea—discovery of dimensional

structure—connects to prior work as a particular case of the more general problem of learning symmetries from data (Benton et al., 2020; Cahill et al., 2020).

2. Units and dimensions

Almost every physical quantity (any position, velocity, or energy, say) has units (inches, kilometers per hour, or BTUs, say). In the physical sciences we are advised to use SI units (Thompson and Taylor, 2008), which include meters (m), meters per second (m s^{-1}), and Joules (J), for example. Any energy can be converted to J, any velocity can be converted to m s^{-1} , and so on, according to known conversion factors. There are dimensionless quantities in physics too, such as Reynolds numbers, or concentrations, but these can also be thought of as having units of unity (or percent or parts per million or so on).

Abstracting slightly, all the (say) SI units are built on *base units* of kilograms (kg), meters (m), seconds (s), kelvin (K), amperes (A), and a few others (such as moles). That is, it is possible to convert any SI unit into powers of the base units. For example, a pascal (Pa) is a $\text{kg m}^{-1} \text{s}^{-2}$, and a volt (V) is a $\text{kg m}^2 \text{s}^{-3} \text{A}^{-1}$. That is, the units of any physical quantity can be converted to powers of the SI base units.

Abstracting even further, there is a concept of dimensions, which is the generalization of units, or the thing that is unchanged when you change the units of something. Two energies, even if measured in different unit systems, both have the *dimensions* of energy. In this sense, there are not just the *base units* of kg, m, s, K, A, and so on; there are also the *base dimensions* of mass, length, time, temperature, current, and so on. That is, any energy can be expressed as a product of a mass times two powers of a length divided by two powers of a time. Or, said another way, an energy can be divided by a mass, divided by two powers of length, and multiplied by two powers of time to deliver a dimensionless quantity. It is always possible to create, from any dimensioned quantity, a dimensionless quantity by multiplying and dividing (carefully chosen) powers of quantities with the base dimensions.

Physical law (and indeed all general relationships among things) obey dimensional rules: Only objects with the same dimensions can be added or subtracted. And when two objects are multiplied (or divided), the resulting quantity has the product (or ratio) of the dimensions of the two input objects. These rules are powerful! For example, we used them to derive, in the first Section of this paper, the dependence on mass and length of the period of a simple pendulum, without (directly) employing any equations or physical model.

Not only is it the case that physical quantities that are added must have the same *dimensions*. In detail, the *numerical* addition of the quantities must be performed only after they have been converted to the same *units* as well. And the products (or ratios) of quantities of units will have the products (or ratios) of the input-quantity units.

There is also a concept of having well-defined and consistent base units: For example, imagine having a mass M measured in grams, a length L measured in inches, a force F measured in newtons, and a speed V measured in kilometers per hour. These quantities have inconsistent base units, in the sense that the time unit inside the force unit is not the same as the time unit inside the speed unit. Naive multiplication of different combinations of these quantities will produce outputs with incommensurate units. They have to be converted to consistent units prior to any arithmetic manipulations. This consistency of the base units is sometimes called *coherence* or *units coherence*. In what follows, we will assume (and later

require) that the inputs and outputs of any model or problem under consideration has been converted into coherent units, for example the explicitly coherent SI system (Thompson and Taylor, 2008).

Coherence is a hard requirement, but still leaves a lot of room to maneuver. For example, in one of the examples in Section 7, we measure horizontal distances in meters and volumes of water in liters. These are incoherent technically, since a volume can be expressed as a length cubed. However, since we express the problem such that horizontal distances and volumes never inter-convert, we can coherently express the problem with this choice.

Sometimes physicists like to work with dimensionless problems in which nothing in the problem has dimensions. How is this achieved? This is only possible when the problem considered exhibits unique natural or fundamental scales that have (or can be combined to have) dimensions of the relevant base dimensions. For example, in cosmological problems, the speed of light, the gravitational constant, and the Hubble constant can be combined to deliver a well-defined fundamental mass scale, length scale, and time scale. Once these are defined, many dimensional quantities can be made dimensionless by scaling out these fundamental scales. This operation—of making a dimensional problem dimensionless by using fundamental scales—is supported theoretically by the Buckingham Pi Theorem (Buckingham, 1914) and motivates this work.

3. Definitions

We consider spaces $\mathcal{Z} = \prod_{i=1}^d \mathcal{X}_{\mathbf{u}_i}$, which consist of coherent (meaning described in a consistent units system) dimensional elements. Each factor $\mathcal{X}_{\mathbf{u}_i}$ is a space of values for a given feature, which is measured in units specified by a parameter \mathbf{u}_i . Thus $x_1 \in \mathcal{X}_{\mathbf{u}_1}$ might be a mass, $x_2 \in \mathcal{X}_{\mathbf{u}_2}$ a temperature, $x_3 \in \mathcal{X}_{\mathbf{u}_3}$ a velocity, etc. As a set, each $\mathcal{X}_{\mathbf{u}_i}$ is just \mathbb{R} , but the specification of its dimensions via \mathbf{u}_i endows it with a specific action by a group G of rescalings. A precise development of this setup follows.

We fix a list of k base units in terms of which all the desired features can be described. For example, if the features consist of energies, temperatures, velocities, forces, masses, and accelerations, the base units could be (kg, m, s, K) (and $k = 4$). The choice of base units determines a *rescaling group* $G := \mathbb{R}_{>0}^k$. An element $(g_1, \dots, g_k) \in G$ rescales the i th base unit by a factor of g_i for each i .

Say there are d features. Then for each $i = 1, \dots, d$, we express the units of the i th feature in terms of the base units, and record this expression in an integer vector $\mathbf{u}_i \in \mathbb{Z}^k$, whose j th component is the exponent to which the j th base unit occurs in this expression. Continuing the example, if the first feature is an energy measured in Joules, then $\mathbf{u}_1 = [1, 2, -2, 0]$, because $1 \text{ J} = 1 \text{ kg m}^2/\text{s}^2$. We then define $\mathcal{X}_{\mathbf{u}_i}$ to be the real line \mathbb{R} equipped with the action by G induced by its action on the base units. Explicitly, if $x_i \in \mathcal{X}_{\mathbf{u}_i}$ and $g = (g_1, \dots, g_k) \in G$, then the action is given by the formula

$$g \cdot x_i = \left(\prod_{j=1}^k g_j^{-u_{ij}} \right) x_i. \tag{1}$$

In our running example, if we replace kg with g and m with cm, leaving s and K untouched, then the group element that accomplishes this rescaling is $g = (0.001, 0.01, 1, 1)$, and if

$x_1 = 2.9$, representing a value of 2.9 J, then

$$g \cdot x_1 = (0.001)^{-1}(0.01)^{-2}(1)^2(1)^0(2.9) = 2.9 \times 10^7$$

reflecting the fact that $2.9 \text{ J} = 2.9 \times 10^7 \text{ g cm}^2/\text{s}^2$.

The space of features is then the cartesian product

$$\mathcal{Z} = \prod_{i=1}^d \mathcal{X}_{\mathbf{u}_i}. \quad (2)$$

It is a real vector space under coordinatewise addition and multiplication by (dimensionless) scalars. Furthermore, because each factor carries an action by the rescaling group G , the space \mathcal{Z} does as well. Note that the action is completely specified by the ordered list $(\mathbf{u}_1, \dots, \mathbf{u}_d) \in (\mathbb{Z}^k)^d$ of units vectors. Sometimes we will denote $\mathbf{x} \in \mathcal{Z}$ as $\mathbf{x} = (x_i, \mathbf{u}_i)_{i=1, \dots, d}$ to indicate the units of each of its features. We call such a \mathcal{Z} a **units-typed space**, and a function between units-typed spaces a **units-typed function**.

Definition 1 *If a units-typed function $f : \mathcal{Z}_X \rightarrow \mathcal{Z}_Y$ has the property that*

$$f(g \cdot x) = g \cdot (f(x)) \quad (3)$$

*for every $g \in G$, then f is a **units-equivariant function**.*

In order for a function f to be units-equivariant, it will be necessary that each of the output exponent vectors of \mathcal{Z}_Y lies in the span of the set of input exponent vectors of \mathcal{Z}_X .

Finally, we point out that in addition to \mathcal{Z} being a real vector space, elements of $\mathcal{X}_{\mathbf{u}}$ can be multiplied by elements of $\mathcal{X}_{\mathbf{u}'}$. In summary the algebraic rules for $x \in \mathcal{X}_{\mathbf{u}}$ and $x' \in \mathcal{X}_{\mathbf{u}'}$, $\alpha \in \mathbb{R}$ and $\gamma \in \mathbb{Z}$ are the following:

$$\alpha(x, \mathbf{u}) = (\alpha x, \mathbf{u}), \text{ where } \alpha \text{ is a dimensionless scalar} \quad (4)$$

$$(x, \mathbf{u}) + (x', \mathbf{u}') = \begin{cases} (x + x', \mathbf{u}) & \text{if } \mathbf{u} = \mathbf{u}' \\ \text{does not exist} & \text{otherwise} \end{cases} \quad (5)$$

$$(x, \mathbf{u})(x', \mathbf{u}') = (xx', \mathbf{u} + \mathbf{u}') \quad (6)$$

$$(x, \mathbf{u})^\gamma = (x^\gamma, \gamma \mathbf{u}), \text{ where } \gamma \text{ is a (dimensionless) integer.} \quad (7)$$

4. Units-equivariant regressions

Given training data $(\mathbf{x}_t, \mathbf{y}_t)_{t=1, \dots, N}$, where $\mathbf{x}_t \in \mathcal{Z}_X$ and $\mathbf{y}_t \in \mathcal{Z}_Y$ (both units-typed spaces), a units-equivariant regression is a regression restricted to a space of units-equivariant functions.

There are multiple approaches for imposing exact symmetries on machine learning methods. Here we take an invariant-features approach (Villar et al., 2021). We begin by algorithmically constructing a featurizer $\phi(\cdot)$ that constructs dimensionless features ξ from the dimensioned input data \mathbf{x} , and a decoder $g_{\mathbf{x}, \mathbf{v}}(\cdot)$ that converts dimensionless label predictions $\hat{\eta}$ into dimensioned training-label predictions $\hat{\mathbf{y}}$ with dimensions of \mathbf{v} . See Figure 1 for a visualization of the setup.

Regression (or classification, or any other task) proceeds as usual, but in the space of purely dimensionless features and labels, with the dimensioned training labels appearing only

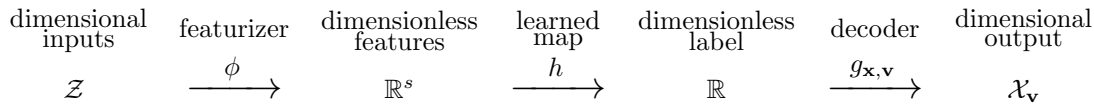


Figure 1: Overview of the general approach.

in the cost function. The concept underlying this approach is that, for the units equivariance to be exact, it is necessary that the inputs to any method that implements nonlinear functions of the input \mathbf{x} (such as a multilayer perceptron, or a kernel regression) act instead only on dimensionless features ξ , because otherwise the nonlinearities effectively (internally) add and subtract quantities with different dimensions, which violates the equivariance. This approach borrows ideas from the Buckingham Pi Theorem (Buckingham, 1914), and uses technology from linear algebra over the integers (Stanley, 2016) to construct the featurizer $\phi(\cdot)$ algorithmically.

Specifically, the input space \mathcal{Z} includes d dimensional input features, such as mass, temperature, etc (2). Some of the inputs will be fundamental constants, such as Newton’s constant, speed of light, etc. The featurizer $\phi : \mathcal{Z} \rightarrow \mathbb{R}^s$ delivers s (dimensionless) products of integer powers of the numerical elements of \mathcal{Z} . If $\mathbf{x} = (x_i, \mathbf{u}_i)_{i=1, \dots, d}$ then $\phi(\mathbf{x}) = (\phi_1(\mathbf{x}), \dots, \phi_s(\mathbf{x}))$ where for all $j = 1, \dots, s$ we have

$$\xi_j = \phi_j(\mathbf{x}) = \prod_{i=1}^d x_i^{\alpha_{ji}} \text{ where } \sum_{i=1}^d \alpha_{ji} \mathbf{u}_i = \mathbf{0} \in \mathbb{Z}^k, \quad (8)$$

where the constraint guarantees that ξ_j is dimensionless. The exponents $\alpha_{ji} \in \mathbb{Z}$ can be found by solving the system of diophantine linear equations in (8) and the solutions form a lattice, the dimension of which can be computed as:

$$\#\text{dimensionless features} = \#\text{input variables} - \#\text{independent units}, \quad (9)$$

where the number of *independent* units coincides with the number of linearly independent vectors in $\{\mathbf{u}_i\}_{i=1}^d$. For example, consider three velocities v_1, v_2, v_3 with units m s^{-1} , the number of units is two (m and s), but the number of independent units is one, making the dimensionless scalars a two-dimensional lattice.

We could select our featurizer to produce a basis of the lattice (we use the Smith Normal Form to this end (Stanley, 2016), a similar approach to (Hubert and Labahn, 2012), which uses the Hermite Normal Form), or we could select our featurizer to produce all lattice points within a bounded region.

If the dimensioned output is $\mathbf{y} = (y, \mathbf{v}) \in \mathcal{X}$ we find an integer solution α_{yi} of $\sum_{i=1}^d \alpha_{yi} \mathbf{u}_i = \mathbf{v}$ and the decoder $g_{\mathbf{x}, \mathbf{v}} : \mathbb{R} \rightarrow \mathcal{X}$ is $g_{\mathbf{x}, \mathbf{v}}(\hat{\eta}) = \hat{\eta} \prod_{i=1}^d x_i^{\alpha_{yi}}$. In words, the decoder finds from \mathbf{x} a product of integer powers of elements of \mathbf{x} that has the same dimensions as the output label \mathbf{y} , and multiplies the dimensionless label prediction $\hat{\eta}$ by that product. This is possible because any units-equivariant function must have the exponent vector \mathbf{v} lie in the span of the input vectors $\{\mathbf{u}_i\}_{i=1}^d$.

The training of a regression model usually involves optimization of a loss function. This is often a norm of a difference between the training labels \mathbf{y} and their predictions $\hat{\mathbf{y}}$. When the problem is made dimensionless, this loss can be made dimensionless as well, or else it can

be left dimensional. In many contexts the loss is a chi-squared objective or a log-likelihood, or can be interpreted as such. In these cases the loss is dimensionless naturally. The units-equivariance approach we recommend is agnostic to whether the loss is dimensionless or dimensional; adoption of this approach does not require adoption of any particular loss.

This approach does, however, place several significant burdens on the user: All elements of the input \mathbf{x} and output \mathbf{y} of the method must have well-defined and known units, and the units information must be encoded in the form of a k -vector of integer powers of a well-defined list of k base units. Also, sometimes quantities external to the natural training data must be included with the inputs \mathbf{x} , such as parameters or fundamental constants (such as Newton’s constant and the speed of light), that are relevant to unit conversions or natural relationships among quantities with different units.

The key idea is that the dimensionless featurizer $\phi(\cdot)$, which produces s dimensionless features, can be compared with an arbitrary featurizer $\tilde{\phi}(\cdot)$, which produces p features that are not necessarily dimensionless. For example, we can consider the space spanned by rational monomials of inputs of a certain degree.

Definition 2 (Rational monomial) *A function $P : \mathbb{R}^d \rightarrow \mathbb{R}$ is a **rational monomial** (also known as a **Laurent monomial**) if*

$$P(x_1, \dots, x_d) = \prod_{i=1}^d a_i x_i^{\alpha_i}, \quad (10)$$

where the coefficients $a_i \in \mathbb{R}$ and the exponents $\alpha_i \in \mathbb{Z}$. The degree of P is defined as $\sum_{i=1}^d |\alpha_i|$.

The units-equivariance approach (8) will produce features consisting of dimensionless rational monomials (example: $\text{mass} * \text{spring constant} * (\text{length})^2 * (\text{momentum})^{-2}$ is a dimensionless rational monomial), whereas a non-equivariant approach can produce arbitrary features of the same type (rational monomials of bounded degrees). We claim that imposing the units equivariance provides the correct inductive bias for the learning problem. In Section 5 we briefly discuss the generalization gains of imposing this exact symmetry.

This approach plays well with many machine learning approaches, including linear regression, kernel regression, and deep learning: It involves only a swap-in replacement for the featurizing or feature normalization that is usually done prior to training a model, and a tweak to the output layer of the method. Thus it can be adapted to almost any machine learning methods in use at the present day.

5. Bias, variance, and generalization

Imposing the exact units-equivariance symmetry in regression tasks improves the prediction performance even in cases where the held out data has out-of-distribution properties. This empirical improvement can be partly attributed to the fact that the symmetry acts like a physics-informed prior which constraints the regression inputs to satisfy correct dimensional scaling relationships. Another reason is due to dimensionality reduction: when the task is made dimensionless the resulting number of independent, dimensionless inputs is always strictly less than the number of dimensional inputs. Therefore, at fixed model complexity

(e.g. rational monomials of a certain degree), the number of free parameters or the model capacity goes down when the problem is made dimensionless. A third reason is that the dimensional scalings aid out-of-distribution generalization, because there are many very different distributions (e.g., for the features) in the dimensional inputs that map to the same distribution in dimensionless quantities. This observation is corroborated in related literature where different types of equivariances are shown related to data augmentation procedures (Chen et al., 2020a), which, in turn, lead to empirically favorable performance in out-of-distribution settings (Liang and Zou, 2022).

These considerations lead to problem-dependent improvements. In what follows, we focus on linear combinations of rational monomials—where the featurizer and decoder (Section 4) construct rational monomials of the task inputs.

Model capacity In the rational monomial context, let X be an $n \times p$ matrix made up of rational monomials of the input dimensional features, where n is the number of training-data examples and p is the number of rational monomials. In the standard linear regression setting, consider a $n \times 1$ set of labels Y , $Y = [y_1, \dots, y_n]^\top$, related to X through the linear form $y_i = x_i^\top \beta + \epsilon_i$, with $\epsilon_i \sim \mathcal{N}(0, \sigma^2)$. We consider two cases: one (naive) in which the feature matrix X is $n \times p$ and contains rational monomials with no regard to their dimensions, and another (dimensionless) in which the feature matrix \bar{X} is $n \times s$ and contains only dimensionless rational monomials.

The linear combinations of rational monomials up to a fixed degree can be imagined as a lattice of integer vectors inside a ball of some norm, because each rational monomial has the inputs taken to integer powers, including negative powers. In this case a third-degree rational monomial, say, would have a norm of three, possibly an $L1$ norm (but there is a choice). If there are d dimensional inputs, the number p of rational monomial terms up to (and including) order r that can be made is equal to the number of lattice points in the unit-cell integer lattice of dimension d inside a d -ball of radius r . Naively, the number p scales as r^d with some prefactor that depends on the norm choice (and d).

The number of dimensionless rational monomials to the same degree is far less. There are two reasons. First, there are $d - k$ independent dimensionless quantities, where k is the number of independent units in play, so the lattice is lower in dimensionality. Second, the lattice of dimensionless quantities has a unit cell that is larger than unity, in general. Thus the number s of dimensionless rational monomial terms scales as r^{d-k} with a small prefactor. In general, in problems of interest, we expect $s \ll p$. Our experiments (Section 7) confirm this expectation.

Bias and Variance We briefly recall the standard notions of bias, variance and risk arising in regression tasks. With the standard min-norm L2 objective, the best-fit coefficient vector $\hat{\beta}$ is given by

$$\hat{\beta} \leftarrow X^\dagger Y, \quad (11)$$

$$X^\dagger = \begin{cases} (X^\top X)^{-1} X^\top & \text{for } n > p \\ X^\top (X X^\top)^{-1} & \text{for } n < p \end{cases} \quad (12)$$

where X^\dagger is the pseudo-inverse of X . The cost function in the naive case is the standard L2 loss $\|Y - X\beta\|_2^2$. In the dimensionless case, the cost function is $\|Y - g_{X,Y}(\bar{X}\beta)\|_2^2$, where

$g_{X,Y}()$ is the decoder function (see above) which multiplies each element of $\bar{X} \beta$ by a rational monomial of the inputs. The resulting dimensionless $\bar{X} \beta$ matches the size the labels Y . Further, the associated *risk* R or expected mean-squared error on held-out test data, can be decomposed in a squared-bias term and a variance term of the form

$$R = \underbrace{\beta^\top \Pi \Sigma \Pi \beta}_{\text{squared bias}} + \underbrace{\frac{\sigma^2}{n} \text{tr}(\hat{\Sigma}^\dagger \Sigma)}_{\text{variance}} + \sigma^2 \quad (13)$$

where $\hat{\Sigma} = \frac{1}{n} X^\top X$ is the empirical variance tensor, $\Pi = I - \hat{\Sigma}^\dagger \hat{\Sigma}$ is a projection operator, β is the true coefficient vector, and $\hat{\Sigma}^\dagger$ is the pseudo-inverse of $\hat{\Sigma}$. For more discussion of the assumptions underlying such expressions, see, for example Hastie et al. (2019).

For our purposes, the most important assumption is that the true β exists! That is, the true relationship between X and Y is contained within the scope of the feature space. Under this assumption, the bias usually vanishes when $p < n$, or when the empirical variance $\hat{\Sigma}$ is full rank. This regime is called the under-parameterized regime. The bias is non-zero when $p > n$. This is called the over-parameterized regime. In this regime, the bias generally increases as p increases. The reduction in model capacity from p in the naive case to s in the dimensionless case (with $s \ll p$) thus enormously decreases the bias. Either the reduction from p to s takes the problem from over-parameterized to under-parameterized, and thus eliminates the bias entirely, or else it reduces the bias within the over-parameterized regime.

Similarly, the reduction in model capacity from p to s (with $s \ll p$) will also generally decrease the variance of the estimator. Thus the variance is also expected to be reduced when the problem is made dimensionless. As we just noted, this all depends critically on the true model being in the space of linear combinations of the rational monomials, and the true model obeying the units equivariance.

Out-of-distribution generalization The exact scaling symmetries enforced by the units equivariance extend to arbitrary dilations of the base dimensions. Thus they connect function outputs for very different inputs. In the context of regression this means that the predictions of trained units-equivariant models ought enable accurate predictions far outside the domain of the training set. One way to state this is to compare the domains of the dimensionless features to the domains of the raw dimensional features.

Mathematically, this can be stated in terms of out-of-distribution generalization (Arjovsky, 2020; Geisa et al., 2021; Dey et al., 2022). In particular, consider a generic problem with d inputs with dimensions made from k base units, and (therefore) a basis of $s = d - k$ dimensionless quantities. Consider a training set sampled from a distribution μ supported in a compact set $\mathcal{D} \subset \mathbb{R}^d$. This induces a distribution $\phi(\mu)$ in the space of dimensionless features \mathbb{R}^s . Many distributions in \mathbb{R}^d (possibly even supported in disjoint sets) map to $\phi(\mu)$. For a trivial example, consider $d = 2$ mass inputs, such that $k = 1$; if the training set has masses in kg drawn from $\text{Unif}(0, 1)$ and the test set has masses in g drawn from $\text{Unif}(0, 10^4)$, they will nonetheless both have the same distribution in the one ($d - k = 1$) available independent dimensionless quantity (the ratio of masses). This is one reason why this method allows us to generalize to settings that can be considered out-of-distribution in the original input space. We conjecture that the out-of-distribution generalization improvement spans beyond this trivial case. We show numerical evidence of this claim in Section 7. We believe that a rigorous

out-of-distribution result could be formalized using techniques from domain adaptation and meta-learning (Ben-David et al., 2010; Mansour et al., 2009; Hanneke and Kpotufe, 2019; Li et al., 2018; Kang and Feng, 2018); we leave that for future work.

6. The geometry of invariant function spaces

Recent results show how to compute explicitly the gains in terms of generalization gaps and sample complexity of imposing group invariances and equivariances in machine learning. The results from Mei et al. (2021) and Bietti et al. (2021) hold for finite groups, whereas the results from Elesedy and Zaidi (2021) and Elesedy (2021) hold for general compact groups. Specifically, Elesedy and Zaidi (2021) shows that if we are aiming to learn a target invariant function f^* from samples from an invariant distribution μ , then for any estimator \hat{f} , the projection of \hat{f} onto the space of invariant functions has smaller expected error. We explain the details below, in this Section.

The problem we consider here, units equivariance, uses the group of scalings, which is unfortunately non-compact so the results from Elesedy and Zaidi (2021) don't directly apply. In particular given a function, it is unclear what is the *correct* notion of its projection onto the space of invariant functions? This is particularly relevant because our approach does not compute a regression to later project its estimator onto the space of invariant functions. It directly solves a regression in a space of invariant functions. The question of how much does one gain by using this approach assumes the existence of a certain non-invariant baseline.

There are two notions of projection we consider, (1) the so-called Reynolds projection, which generalizes the notion of averaging the function along the group orbit, (2) the orthogonal projection with respect to the measure μ used to generate the data. In the case of compact groups and data sampled from invariant measures both notions coincide, giving a very simple expression for the generalization gap of a function in comparison with its projection onto the space of invariant functions. However, we will see that in the non-compact case, the notions do not coincide for any real measure μ .

In the rest of this section we

- Summarize the ideas from Elesedy and Zaidi (2021) that allow them to compute a generalization gap for compact groups.
- Explain how to extend those techniques to non-compact groups using the Weyl's trick.
- Show that if we replace \mathcal{X} with a complex domain, and the measure is invariant with respect to complex scalings of modulus 1, then the results from Elesedy and Zaidi (2021) hold.
- Show that if the domain is real, the two notions of projection don't match for any choice of measure.

Projections onto invariant functions We first explain ideas from Elesedy and Zaidi (2021) developed in the context of invariant and equivariant functions with respect to actions by compact groups.

Given $X \subseteq \mathbb{R}^d$ and G a compact group acting on X , we fix a G -invariant measure μ . We consider the Hilbert space of functions $\mathcal{H} = \mathcal{L}_2(X, \mu)$. The action of G on X induces a

natural action on \mathcal{H} via the formula

$$[\lambda \cdot f](x) := f(\lambda^{-1} \cdot x)$$

for $x \in X$ and $\lambda \in G$. We split \mathcal{H} into two orthogonal components, the closed *ground-truth* G -invariant subspace $\bar{\mathcal{H}}$ consisting of the functions $f \in \bar{\mathcal{H}}$ satisfying $\lambda \cdot f = f$ for all $\lambda \in G$, and its orthogonal complement \mathcal{H}^\perp , so that $\mathcal{H} = \bar{\mathcal{H}} \oplus \mathcal{H}^\perp$. Using that μ is G -invariant, it is noted (Elesedy and Zaidi, 2021) that the orthogonal projection onto $\bar{\mathcal{H}}$ coincides with averaging along the G -orbit, also known as the Reynolds operator:

$$\mathcal{O}f(x) = \int_G f(\lambda \cdot x) d\lambda, \quad (14)$$

where λ is the normalized Haar measure of the group. The Reynolds operator has good algebraic properties. It can be alternatively characterized as the unique G -invariant projection $\mathcal{H} \rightarrow \bar{\mathcal{H}}$, i.e., the unique linear map $\mathcal{O} : \mathcal{H} \rightarrow \bar{\mathcal{H}}$ that restricts to the identity on $\bar{\mathcal{H}}$ and satisfies

$$\mathcal{O}(\lambda \cdot f) = \mathcal{O}f \quad (15)$$

for $\lambda \in G$ and $f \in \mathcal{H}$. Yet another characterization is that it restricts to the identity on any subspace consisting of invariants, and to zero on any G -stable subspace not containing nontrivial invariants. The Hilbert space \mathcal{H} contains the algebra of compactly-supported continuous functions $C_c(X)$ as a dense subspace, and the Reynolds operator has the property that its restriction to this algebra commutes with multiplication by invariant such functions, i.e., it satisfies

$$\mathcal{O}(fh) = f\mathcal{O}h \quad (16)$$

for all $f \in C_c(X)^G$ (the subalgebra of invariant compactly-supported continuous functions) and $h \in C_c(X)$. In other words, \mathcal{O} restricts to a $C_c(X)^G$ -module projection $C_c(X) \rightarrow C_c(X)^G$. Given f we have $\arg \min_{h \in \bar{\mathcal{H}}} \|h - f\|_\mu^2 = \mathcal{O}(f)$. In order to show this, it suffices to observe that \mathcal{O} is self-adjoint with respect to the inner product in $\mathcal{L}_2(X, \mu)$:

$$\langle \mathcal{O}f, h \rangle_\mu = \int_X \left\langle \int_G f(g \cdot x) d\lambda, h(x) \right\rangle d\mu(x) \quad (17)$$

$$= \int_X \int_G \langle f(g \cdot x), h(x) \rangle d\lambda d\mu(x) \quad (18)$$

$$= \int_X \int_G \langle f(x), h(g^{-1} \cdot x) \rangle d\lambda d\mu(x) \quad (19)$$

$$= \langle f, \mathcal{O}h \rangle_\mu. \quad (20)$$

Note that (19) holds due to μ being G -invariant. Under this assumption, this property of \mathcal{O} is to be expected: the G -invariance of μ means that the inner product on $\mathcal{H} = \mathcal{L}_2(X, \mu)$ is also G -invariant, thus G acts by unitary transformations on \mathcal{H} , so the latter's decomposition into irreducible representations of G is an orthogonal decomposition. Because \mathcal{O} annihilates the nontrivial representations, it thus amounts to orthogonal projection to the space of invariants.

Now, given $f^* : X \rightarrow \mathbb{R}^k$, $f^* \in \bar{\mathcal{H}}$ they consider data $y = f^*(x) + \xi$ where ξ is sampled from a zero-mean, finite variance distribution in \mathbb{R}^k . The risk of a function f is the expected value of the prediction error

$$R(f) = \mathbb{E}_{x \sim \mu} \|y - f(x)\|_2^2 \tag{21}$$

and given two functions f and f' the generalization gap is

$$\Delta(f, f') = R(f) - R(f'). \tag{22}$$

In Elesedy and Zaidi (2021) a regression problem is considered in which the regression is performed on a subspace $U \subset \mathcal{H}$ that is closed under (14). Then U can be decomposed into closed subspaces $U = \bar{U} \oplus U^\perp$ where $\bar{U} \subset \bar{\mathcal{H}}$ and $U^\perp \subset \mathcal{H}^\perp$. Given a function $f \in U$, let $\bar{f} := \Pi_{\bar{U}} f$ and $f^\perp := \Pi_{U^\perp} f$ the respective orthogonal projections of f . Note that under the present hypothesis $\bar{f} := \mathcal{O}f$ and $f^\perp := f - \mathcal{O}f$? since \mathcal{O} restricted to U is the orthogonal projection to \bar{U} .

The goal is to compute $\Delta(f, \bar{f})$, namely what is the excess risk of doing the regression on the function space U instead of restricting to the invariant subspace \bar{U} , which corresponds to the ground truth. A simple computation shows that if x is sampled from μ , then

$$\Delta(f, \bar{f}) = \|f^\perp\|_\mu^2, \tag{23}$$

this in particular shows that there is always a benefit to restricting to the ground truth subspace. For instance if the target is a group invariant function, and we do a regression in a space of polynomials, we might as well restrict the regression to group invariant polynomials, since the generalization error will be strictly smaller.

The rest of the analysis in Elesedy and Zaidi (2021) focuses on computing $\|f^\perp\|_\mu^2$ for data models, for instance, assuming U is the space of linear functions (they discussed both over and under parameterized), and the input is Gaussian with mean zero and identity covariance (assuming the spherical Gaussian distribution is G -invariant). A slightly more general formulation allows them to express the same ideas for equivariance. This work has been extended to kernel regressions (Elesedy, 2021).

Reynolds projection onto scaling invariant functions via Weyl’s unitarian trick

Let $\mathcal{X} = (\mathbb{R}, \mathbb{Z}^k)^d$ where each of the d features x_i has base units exponents $\mathbf{u}_i = (u_{i1}, \dots, u_{ik}) \in \mathbb{Z}^k$ expressed in terms of k base units. The Buckingham Pi theorem discussed in Section 4 shows that units-equivariant functions are in a one-to-one correspondence with functions of (finitely many) dimensionless features (constructed as products of powers of input features). This characterization also implies that the dimensionless functions are exactly the functions that are invariant with respect to unit rescalings. For each base units, represented here by the index $j \in \{1, \dots, k\}$, we consider u_{ij} , its exponent in each feature x_i . Then f is scaling invariant (i.e. dimensionless¹) if and only if for all $g \in \mathbb{R}_{>0}$ and all $j \in \{1, \dots, k\}$ we have

$$f(g^{u_{1j}} x_1, \dots, g^{u_{dj}} x_d) = f(x_1, \dots, x_d), \tag{24}$$

1. We assume the output is dimensionless for simplicity, without loss of generality a dimensioned output function $F^* : \mathcal{Z} \rightarrow \mathcal{X}_v$ can be obtained as $F^*(\mathbf{x}) = g_{\mathbf{x}, \mathbf{u}}(f^*(\mathbf{x}))$ where $g_{\mathbf{x}, \mathbf{u}}$ is fixed.

this property is also known as self-similarity (Barenblatt, 1996). The rescalings can be seen as an action by the appropriate renormalization group, in this case $G = (\mathbb{R}_{>0})^k$, defined as

$$(g_1, \dots, g_k) \cdot (x_1, \dots, x_d) = \left(\left(\prod_{j=1}^k g_j^{u_{1j}} \right) x_1, \dots, \left(\prod_{j=1}^k g_j^{u_{dj}} \right) x_d \right). \quad (25)$$

Since the group is not compact, the results of Elesedy and Zaidi (2021) are not directly applicable. However, it is closely related to the reductive real algebraic group $(\mathbb{R}^\times)^k$, so some of the concepts can be generalized by using Weyl’s unitarian trick. (This will require us to work in complex space.) However, the key property from Elesedy and Zaidi (2021) in which the Reynolds projection coincides with the orthogonal projection with respect to the measure, will not hold in real space.

We consider U a space of real analytic functions (for instance, rational monomials). We can define a Reynolds projection to the G -invariant functions \bar{U} , analogous to (14), by using Weyl’s unitarian trick. If $f : \mathbb{R}^d \rightarrow \mathbb{R}$ is a real analytic function it has an analytic continuation, $f_{\mathbb{C}} : \mathbb{C}^d \rightarrow \mathbb{C}$, such that $f_{\mathbb{C}}|_{\mathbb{R}^d} = f$. Weyl’s unitarian trick is to replace the group $G = (\mathbb{R}_{>0})^k$ with the torus $\mathbb{T}^k = \{\mathbf{z} \in \mathbb{C}^k : |z_i| = 1\}$. Both groups are Zariski-dense in the group $(\mathbb{C}^\times)^k$ —in other words, any polynomial that vanishes identically on either G or \mathbb{T}^k actually vanishes identically on all of $(\mathbb{C}^\times)^k$ —and it follows, because the group action (25) is described by rational functions, that all three groups have the same invariants. On the other hand, the torus \mathbb{T}^k is compact, so we can average over it to obtain a projection

$$\mathcal{Q}f(x_1, \dots, x_d) = \int_{\mathbb{T}^k} f_{\mathbb{C}}((z_1, \dots, z_k) \cdot (x_1, \dots, x_d)) d\lambda_{\mathbb{C}}(\mathbf{z}), \quad (26)$$

where the Haar measure $\lambda_{\mathbb{C}}$ coincides with the (normalized) Lebesgue measure on the torus—namely, the Lebesgue measure scaled by $\frac{1}{(2\pi)^k}$.

In order to explain how the projection \mathcal{Q} behaves, we first note that the rational monomials define characters for the group action. Namely,

$$\mathbf{x}^{\mathbf{a}} = \prod_{i=1}^d x_i^{a_i}, \quad (z_1, \dots, z_k) \cdot \mathbf{x}^{\mathbf{a}} = \left(\prod_{j=1}^k z_j^{\sum_{s=1}^k u_{sj} a_j} \right) \mathbf{x}^{\mathbf{a}}, \quad (27)$$

therefore

$$\chi_{\mathbf{x}^{\mathbf{a}}} : (\mathbb{C}_{>0})^k \rightarrow \mathbb{C}_{>0} \quad (28)$$

$$(z_1, \dots, z_k) \mapsto \prod_{j=1}^k z_j^{\sum_{s=1}^k u_{sj} a_j} \quad (29)$$

is a continuous group homomorphism (same for the real characters). Therefore, the rational monomials are eigenvectors of \mathcal{Q}

$$\mathcal{Q}(\mathbf{x}^{\mathbf{a}}) = \int_{\mathbb{T}^k} \mathbf{z} \cdot \mathbf{x}^{\mathbf{a}} \lambda_{\mathbb{C}}(\mathbf{z}) = \int_{\mathbb{T}^k} \chi_{\mathbf{x}^{\mathbf{a}}}(\mathbf{z}) \mathbf{x}^{\mathbf{a}} \lambda_{\mathbb{C}}(\mathbf{z}) = \mathbf{x}^{\mathbf{a}} \int_{\mathbb{T}^k} \chi_{\mathbf{x}^{\mathbf{a}}}(\mathbf{z}) \lambda_{\mathbb{C}}(\mathbf{z}). \quad (30)$$

A standard computation shows that if χ is a character of a compact group with Haar measure λ , then $\int_G \chi(g) d\lambda = \lambda(G)$ if χ is trivial, and 0 otherwise. In particular this shows

$$\mathcal{Q}(\mathbf{x}^{\mathbf{a}}) = \begin{cases} \mathbf{x}^{\mathbf{a}} & \text{if } \sum_{s=1}^k u_{sj} a_j = 0 \text{ for all } j = 1, \dots, k \\ 0 & \text{otherwise.} \end{cases} \quad (31)$$

In other words, comparing (31) with (8), a rational monomial is either invariant under the group action (i.e. dimensionless), or it is in the kernel of \mathcal{Q} . Thus \mathcal{Q} is a Reynolds operator for the group of scalings.

Generalization gap for (complex) units equivariant regressions In order to use the results from Elesedy and Zaidi (2021) it is not enough to have a projection \mathcal{Q} . We need \mathcal{Q} to be an orthogonal projection in an \mathcal{L}_2 space. To this end, we consider a space of functions of the original input features, where the units equivariant functions are a linear subspace. The characterization from dimensional analysis discussed above suggests to focus on rational monomials. Unfortunately the rational monomials may have poles when features are zero, so in order to define the inner product we will restrict the measure μ to have bounded support which does not include zero. In particular we can consider $X^d = ([-b, -a] \cup [a, b])^d$, and μ the standard (Lebesgue) measure in \mathbb{R}^d restricted to X^d and 0 outside X . We let $\mathcal{H} = \mathcal{L}_2(\mathbb{R}^d, \mu)$. We note that μ is not scaling invariant, and indeed, no compactly-supported measure is scaling-invariant. Relatedly, \mathcal{Q} is not an orthogonal projection in $\mathcal{L}_2(\mathbb{R}^d, \mu)$ for any real measure μ . But we will make it work.

Since we extended the class of functions to a complex domain to use Weyl's trick, we also need to extend the measure μ to $\mu_{\mathbb{C}^d}$. We consider the Lebesgue measure in \mathbb{C}^d with support $(X_{\mathbb{C}})^d$ where $X_{\mathbb{C}} = \{z \in \mathbb{C} : a < |z| < b\}$. Now $\mathcal{H}_{\mathbb{C}} = \mathcal{L}_2(\mathbb{C}^d, \mu_{\mathbb{C}^d})$. We will see that even though $\mu_{\mathbb{C}^d}$ is a complex analog of μ , the resulting Hilbert spaces are not necessarily comparable. In particular \mathcal{Q} is an orthogonal projection in $\mathcal{L}_2(\mathbb{C}^d, \mu_{\mathbb{C}^d})$, due to the fact that $\mu_{\mathbb{C}^d}$ is rotationally symmetric (i.e., invariant under the action by \mathbb{T}^d).

Proposition 3 *If $U \subseteq \mathcal{H}_{\mathbb{C}}$ is a linear subspace closed under scalings, then \mathcal{Q} defined in (26) is the orthogonal projection onto the space of scaling invariant functions. In particular $U = \bar{U} \oplus U^{\perp}$ where $\bar{U} = \text{Image}(\mathcal{Q})$ and $U^{\perp} = \text{kernel}(\mathcal{Q})$.*

Proof It suffices to show: (a) $\mathcal{Q}(U) \subset U$. (b) f is scaling invariant if and only if $\mathcal{Q}(f) = f$. (c) \mathcal{Q} is self adjoint for $\langle \cdot, \cdot \rangle_{\mu_{\mathbb{C}^d}}$. This can be shown with a similar argument to (17)-(20):

$$\langle \mathcal{Q}f, h \rangle_{\mu_{\mathbb{C}^d}} = \int_{X_{\mathbb{C}}^d} \left\langle \int_{\mathbb{T}^k} f(\mathbf{z} \cdot \mathbf{x}) d\lambda_{\mathbb{C}}(\mathbf{z}), h^*(\mathbf{x}) \right\rangle d\mu_{\mathbb{C}^d}(\mathbf{x}) \quad (32)$$

$$= \int_{X_{\mathbb{C}}^d} \int_{\mathbb{T}^k} \langle f(\mathbf{z} \cdot \mathbf{x}), h^*(\mathbf{x}) \rangle d\lambda_{\mathbb{C}}(\mathbf{z}) d\mu_{\mathbb{C}^d}(\mathbf{x}) \quad (33)$$

$$= \int_{X_{\mathbb{C}}^d} \int_{\mathbb{T}^k} \langle f(\mathbf{x}), h^*(\mathbf{z}^{-1} \cdot \mathbf{x}) \rangle d\lambda_{\mathbb{C}}(\mathbf{z}) d\mu_{\mathbb{C}^d}(\mathbf{x}) \quad (34)$$

$$= \langle f, \mathcal{Q}h \rangle_{\mu_{\mathbb{C}^d}}, \quad (35)$$

where h^* is the complex conjugate of h . Note that (34) holds because the measure $\mu_{\mathbb{C}^d}$ is invariant with respect to scalings in \mathbb{T}^k (namely, $\mu_{\mathbb{C}^d}$ is rotationally symmetric). \blacksquare

Note this argument is not possible for μ . We'll see below that \mathcal{Q} is not self-adjoint with respect to any real inner product.

Our argument in the previous section shows that when U is a space generated by rational monomials, the projection onto \bar{U} is easy to characterize. In particular, a simple computation (Proposition (4)) shows that the complex rational monomials are orthogonal in $\mathcal{L}_2(\mathbb{C}^d, \mu_{\mathbb{C}^d})$.

Proposition 4 *Let U be the space of rational monomials, spanned by*

$$\mathcal{B} := \left\{ \mathbf{x}^{\mathbf{a}} := \prod_{i=1}^d x_i^{a_i} : \mathbf{a} = (a_1, \dots, a_d) \in \mathbb{Z}^d \right\}. \quad (36)$$

Then for all $\mathbf{x}^{\mathbf{a}}, \mathbf{x}^{\mathbf{a}'} \in \mathcal{B}$ with $\mathbf{a} \neq \mathbf{a}'$ we have $\langle \mathbf{x}^{\mathbf{a}}, \mathbf{x}^{\mathbf{a}'} \rangle_{\mu} = 0$.

Proof Let $\mathbf{a} \neq \mathbf{a}'$, then

$$\langle \mathbf{x}^{\mathbf{a}}, \mathbf{x}^{\mathbf{a}'} \rangle_{\mu_{\mathbb{C}^d}} = \int_{X_{\mathbb{C}^d}} \prod_{i=1}^d x_i^{a_i} \bar{x}_i^{a'_i} d\mu_{\mathbb{C}^d} \quad (37)$$

$$= \int_{X_{\mathbb{C}^d}} \prod_{i=1}^d r_i e^{j a_i \theta_i} r_i e^{-j a'_i \theta_i} d\mu_{\mathbb{C}^d}, \quad (38)$$

where $x_i = e^{j\theta_i}$ and $j = \sqrt{-1}$. Now since $\mathbf{a} \neq \mathbf{a}'$ we can choose s such that $a_s \neq a'_s$. Using Fubini-Tonelli's theorem we can write:

$$\langle \mathbf{x}^{\mathbf{a}}, \mathbf{x}^{\mathbf{a}'} \rangle_{\mu_{\mathbb{C}^d}} = \int_{X_{\mathbb{C}^{d-1}}} \prod_{\substack{i=1 \\ i \neq s}}^d r_i e^{j(a_i - a'_i)\theta_i} d\mu_{\mathbb{C}^{d-1}} \int_{X_{\mathbb{C}}} r_s e^{j(a_s - a'_s)\theta_s} d\mu_{\mathbb{C}^1}, \quad (39)$$

where the last term is zero because $a_s \neq a'_s$ and the measure $\mu_{\mathbb{C}^1}$ is rotationally symmetric. \blacksquare

This setting allows to generalize the results from Elesedy and Zaidi (2021) to complex scalings of complex functions.

Proposition 5 *Let $X \sim \mu_{\mathbb{C}^d}$ where $\mu_{\mathbb{C}^d}$ is a rotation invariant distribution in $A \subset \mathbb{C}^d$. Let $Y = f * (X) + \xi \in \mathbb{C}$, where ξ is a random element of \mathbb{C} that is independent of X with zero mean and finite variance, and $f^* : A \rightarrow \mathbb{C}$ is scaling invariant. Then, for any f , the generalization gap satisfies*

$$\Delta(f, \mathcal{Q}f) = \|f^\perp\|_{\mu_{\mathbb{C}^d}}^2. \quad (40)$$

Discussion of real units-equivariant functions Even though some dimensional quantities can be complex, for example electromagnetic field amplitudes in Fourier space, most dimensional quantities are real-valued, and the dimensional scalings are always real, therefore the above theory is not directly applicable.

Unfortunately the analysis above will not hold for the real case. Note that the Reynolds operator defined in (26) is well-defined for real functions and delivers the same projection

in the rational monomials case (i.e. it drops the non-dimensionless rational monomials). However this projection does not correspond to an orthogonal projection with respect to any nontrivial measure μ . One way to see this is by observing that the monomials cannot be orthogonal for the real measure μ . For instance no real measure will satisfy that $\langle x^1, x^3 \rangle_\mu = 0$ because $\langle x^1, x^3 \rangle_\mu = \int x^1 x^3 d\mu = \int x^2 x^2 d\mu = \langle x^2, x^2 \rangle_\mu$.

The underlying question here is, what is the right notion of projection of a real function onto the space of units-equivariant functions? The Reynolds projection is the most natural projection from an algebraic point of view, per the discussion following (14). The orthogonal projection with respect to the \mathcal{L}^2 -norm of the measure of the data is the one corresponding to the estimator risk (21). The fact that these two projections diverge in the present case stems from the fact that the measure from which the data is drawn cannot itself be scaling-invariant. Furthermore, there is no reason to expect that the rational monomials are closed under the orthogonal projection in $\mathcal{L}^2(\mathbb{R}^d, \mu)$.

Note that our algorithm does not perform a projection, it directly optimizes in a space of invariant functions. The generalization gap one may want to investigate is $\Delta(\hat{f}, \bar{f})$ where \hat{f} is the output of a baseline regression, and \bar{f} is our units-equivariant regression. We show specific examples in Section 7.

7. Experimental demonstrations

Symbolic regression: Simple springy pendulum In this example, we consider a pendulum bob of mass m (units of kg) at the end of a linear spring, swinging under the influence of gravity. The total mechanical energy or hamiltonian H (units of $\text{kg m}^2 \text{s}^{-2}$) of this system consists of a kinetic energy and two potential-energy contributions:

$$H = \underbrace{\frac{1}{2} \frac{|\mathbf{p}|^2}{m}}_{\text{kinetic energy}} + \underbrace{\frac{1}{2} k_s (|\mathbf{q}| - L)^2}_{\text{spring potential energy}} - \underbrace{m \mathbf{g}^\top \mathbf{q}}_{\text{gravitational potential energy}}, \quad (41)$$

where \mathbf{p} is the 3-vector momentum of the bob (units of kg m s^{-1}), $|\mathbf{p}|^2 = \mathbf{p}^\top \mathbf{p}$, k_s is the spring constant (units of $\text{N m}^{-1} = \text{kg s}^{-2}$), \mathbf{q} is the 3-vector position of the bob relative to the pivot (units of m), $|\mathbf{q}| = \sqrt{\mathbf{q}^\top \mathbf{q}}$, L is the natural length of the spring (units of m), \mathbf{g} is the acceleration due to gravity (units of m s^{-2}). The natural base units here are the SI base units (kg, m, s), but they could just as easily be (stone, furlong, fortnight).

This is almost the simplest possible physics problem. We honor its simplicity by constructing an extremely simplified symbolic regression: Given samples of the parameters m, k_s, L, \mathbf{g} , the initial conditions \mathbf{p}, \mathbf{q} , and the corresponding values of the hamiltonian H , is it possible to infer the exact functional form of the hamiltonian? The answer is yes, of course; the question is: How much does units equivariance help? The answer is: A lot.

First we observe that, in Newtonian mechanics, the hamiltonian—or total mechanical energy—is a scalar. Thus the hamiltonian can be a function only of scalars and scalar products of the vector and scalar inputs (Villar et al., 2021). We construct all rational scalar monomials of the inputs up to a well-defined degree, including, for example $m k_s |\mathbf{q}| (\mathbf{g}^\top \mathbf{p})^{-2}$, where the vectors $\mathbf{g}, \mathbf{p}, \mathbf{q}$ are implicitly column vectors, $|\mathbf{q}|$ is the magnitude of \mathbf{q} , and $\mathbf{g}^\top \mathbf{p}$ is the scalar (inner) product of \mathbf{g} and \mathbf{p} . For our purposes, the degree of the rational monomial

is the maximum absolute value exponent appearing in the expression, so the example would have degree 2. Then we construct all *dimensionless* rational scalar monomials of the inputs up to the same well-defined degree, including, for example, $m k_s L^2 |\mathbf{p}|^{-2}$, which is also of degree 2 but dimensionless. It turns out that there are far fewer dimensionless rational scalar monomials than rational scalar monomials to any degree.

In detail, the dimensional scalar inputs to our monomial lists are the 9 scalars $m, k_s, L, |\mathbf{g}|, (\mathbf{g}^\top \mathbf{p}), (\mathbf{g}^\top \mathbf{q}), |\mathbf{p}|, (\mathbf{p}^\top \mathbf{q}), |\mathbf{q}|$. We produce all monomials to maximum degree 2 but subject to two additional rules: While we count scalars $|\mathbf{g}|, |\mathbf{q}|$, and $|\mathbf{p}|$ as having degree 1, we count scalars $\mathbf{g}^\top \mathbf{p}$ and $\mathbf{p}^\top \mathbf{q}$ and so on as having degree 2 (so at maximum degree 2, say, they cannot appear squared). We also did not permit the dot products $\mathbf{g}^\top \mathbf{p}$ and $\mathbf{p}^\top \mathbf{q}$ and so on to appear with negative powers (because these inverses can produce unbounded singular values in the design matrix). With these inputs and these rules, there are 286 dimensionless monomials to (only!) degree 2, and 187 500 total monomials (irrespective of dimensions) to degree 2.

Given the enormous difference between 286 and 187 500, it is obvious that units equivariance is incredibly informative. We demonstrate the value experimentally by performing symbolic regressions for the hamiltonian H with two different objectives; one an L2, and the other a LASSO objective. In each case the objective is the norm of the difference between the predicted and true hamiltonian value, but made dimensionless by dividing by the quantity $k_s L^2$, which has units of energy. In the L2 case, 8192 training-set objects are used, and in the LASSO case, 128. Training-set objects are drawn from distributions in $m, k_s, L, \mathbf{g}, \mathbf{p}, \mathbf{q}$, in which the scalars m, k_s, L are drawn from uniforms and the vectors $\mathbf{g}, \mathbf{p}, \mathbf{q}$ are drawn from isotropically oriented unit vectors times magnitudes drawn from uniforms. In both cases, the regression applied to the dimensionless-feature design matrix delivers machine-precision-level errors on held-out data, and linear-fit coefficients that represent the correct formula or expression for the hamiltonian.

Given the number (187 500) of baseline monomials, it is impossible computationally to perform an equivalent baseline comparison. That point alone demonstrates the value of the units-equivariant approach for symbolic-regression-like problems. However, in order to test this, we augment the 286 dimensionless monomials with 500 randomly chosen dimensional monomials and—at these training-set sizes—the symbolic regressions fail: They deliver an order of magnitude worse mean-squared error on held-out test data and they do not find the correct coefficients for the hamiltonian expression. The code is publicly available at Google Colab.²

Emulator: Springy double pendulum Next we consider the task of learning the dynamics of the springy double pendulum, which is a pair of single springy pendula connected with a free pivot³ (Figure 2). The goal here is to predict its trajectory at later times from different initial states. For this task, for each of the realization of the N training data, $m_1, m_2, k_{s1}, k_{s2}, L_1, L_2$ are randomly generated from $\text{Unif}(1, 2)$, as well as the norm of the gravitational acceleration vector \mathbf{g} . Initializations at t_0 of the pendulum positions and momenta are generated as those in Finzi et al. (2021) and Yao et al. (2021). The training

2. See <https://dwh.gg/springy>.

3. The source code is published in <https://github.com/weichiyao/ScalarEMLP/tree/dimensionless>.

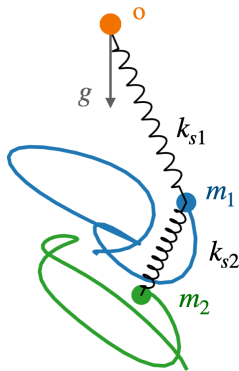


Figure 2: The springy double pendulum.

labels are the positions and momenta at a set of \tilde{T} later times $t \in \{t_1, \dots, t_{\tilde{T}}\}$:

$$\mathbf{z}(t) = (\mathbf{q}_1(t), \mathbf{q}_2(t), \mathbf{p}_1(t), \mathbf{p}_2(t)), \quad t \in \{t_0, \dots, t_{\tilde{T}}\}. \quad (42)$$

In our experiments, the training set consists of positions and momenta of the pendula in a sequence of $\tilde{T} = 10$ equispaced consecutive times sampled from a sequence of $T = 60$ equispaced times obtained by integrating the dynamical system according to its ground truth parameters. In the testing stage, the trajectory at $t = 1, \dots, T$ from different initial states are predicted given the initializations at $t = 0$. We consider three different testing setups to compare the dimensionless scalar-based implementation with the dimensional baseline considered in Yao et al. (2021). This baseline is currently state-of-the-art on this problem. It embodies Hamiltonian and geometric symmetries and performs very well (Yao et al., 2021).

The test data used in Experiment 1 is generated from the same distribution as the training dataset. The test data used in Experiment 2 consists of applying a transformation to the test data in Experiment 1, where each of the input parameters that include a power of kg in its units ($m_1, m_2, k_{s1}, k_{s2}, \mathbf{p}_1(0)$ and $\mathbf{p}_2(0)$) is scaled by a factor randomly generated from $\text{Unif}(3, 7)$. The test data used in Experiment 3 has the input parameters $m_1, m_2, k_{s1}, k_{s2}, L_1$ and L_2 generated from $\text{Unif}(1, 5)$. We use the same training data $N = 30000$ for all three experiments and each test set consists of 500 data points. That is, Experiments 2 and 3 have out-of-distribution test data, relative to their training data.

We implement Hamiltonian neural networks (HNNs; Greydanus et al. 2019; Sanchez-Gonzalez et al. 2019) with scalar-based MLPs for this learning task. In particular, we have a set of scalar inputs $\mathcal{S} = \{m_1, m_2, k_{s1}, k_{s2}, L_1, L_2\}$ and a set of vector inputs $\mathcal{V} = \{\mathbf{g}, \mathbf{p}_1(0), \mathbf{p}_2(0), \mathbf{q}_1(0), \mathbf{q}_2(0) - \mathbf{q}_1(0)\}$. We construct the dimensional scalars (baseline) and dimensionless scalars based on these two sets of inputs.

The dimensional scalar inputs to the baseline MLPs include 32 scalars: (i) scalar inputs \mathcal{S} , as well as their inverses $\{1/a : a \in \mathcal{S}\}$; (ii) inner products of the vector inputs $\{\mathbf{u}^\top \mathbf{v} : \mathbf{u}, \mathbf{v} \in \mathcal{V}\}$, as well as their magnitudes $\{|\mathbf{u}| : \mathbf{u} \in \mathcal{V}\}$.

The dimensionless scalar inputs are the following 32 scalars: (i) $m_1/m_2, k_{s1}/k_{s2}, L_1/L_2$ and their inverses; (ii) we divide each vector input by its magnitude before we compute the inner products, which gives a set of dimensionless scalars $\{(\mathbf{u}^\top \mathbf{v})/(|\mathbf{u}||\mathbf{v}|) : \mathbf{u}, \mathbf{v} \in \mathcal{V}\}$; (iii) we also consider dimensionless rational scalar monomials $(m_i |\mathbf{g}|)/(k_{si} L_i), (k_{si} L_i)/(m_i |\mathbf{g}|)$,

Scalar-based MLPs	Experiment 1	Experiment 2	Experiment 3
Baseline	.0055 ± .0030	.3669 ± .0050	.1885 ± .0031
Dimensionless	.0061 ± .0024	.0089 ± .0034	.0435 ± .0047

Table 1: Geometric mean (standard deviation computed over 10 trials) of state relative errors of the springy pendulum over $T = 60$. Results are shown for the dimensional vs dimensionless scalar-based Hamiltonian Neural Networks (implemented as an MLP) on three different test sets. Test data used in Experiment 1 are generated from the same distribution as the training dataset; test data used in Experiment 2 using the same test data in Experiment 1 but each with its inputs that have units of kg randomly scaled by a factor generated from $\text{Unif}(3, 7)$; test data used in Experiment 3 has mass m , scalar spring constant k_s and natural spring length L generated from a different distribution.

$|\mathbf{q}_i(0)|/L_i$, $|\mathbf{q}_i(0)|^2/L_i^2$, $|\mathbf{p}_i(0)|/(\sqrt{m_i k_{si}} L_i)$, $|\mathbf{p}_i(0)|^2/(m_i k_{si} L_i^2)$, $i = 1, 2$. We use dimensionless scalars as inputs to the MLPs, which makes the outputs of the MLPs also dimensionless. The decoder then scales the outputs to restore the hamiltonian H units of $\text{kg m}^2 \text{s}^{-2}$. At this stage we employ the following 26 scaling factors: $k_{sr} L_i L_j$, $m_i L_j |\mathbf{g}|$, $m_i \mathbf{g}^\top \mathbf{q}_j(0)$, $(\mathbf{p}_i(0)^\top \mathbf{p}_j(0))/m_r$, $k_{sr} \mathbf{q}_i(0)^\top \mathbf{q}_j(0)$, $i, j, r \in \{1, 2\}$, all of which have the units of $\text{kg m}^2 \text{s}^{-2}$.

The dimensional scalars-based and the dimensionless scalars-based MLPs both have equal numbers of model parameters, and are trained with the same set of hyper-parameters (number of training epochs, learning rate, etc.).

The prediction error (or state relative error) at time t is defined as

$$\text{State.RelErr}(t) = \frac{\sqrt{(\hat{\mathbf{z}}(t) - \mathbf{z}(t))^\top (\hat{\mathbf{z}}(t) - \mathbf{z}(t))}}{\sqrt{\hat{\mathbf{z}}(t)^\top \hat{\mathbf{z}}(t)} + \sqrt{\mathbf{z}(t)^\top \mathbf{z}(t)}}. \quad (43)$$

Table 1 reports the average errors over $\{t_1, \dots, t_{60}\}$. When the test data are generated from the same distribution as the training data, the dimensional scalar based MLP exhibits slightly more accurate predictions for longer time scales using the same training hyper-parameters. When we have out-of-distribution test data as in Experiment 2 and 3, the performance of both methods deteriorate as expected, but the dimensionless scalar based MLP exhibits a significantly better generalization performance. In particular, if we rescale the units as in Experiment 2, where all the quantities that have the units of kg are scaled by the same randomly generated factor, the dimensionless scalar based MLP is able to provide comparable performance to results from Experiment 1. Actually, this could be considered to be an in-distribution test set in the space of dimensionless scalars (see Section 5), and thus the only reason why the error is different is because the state relative error (43) is not dimensionless. In other words, our experiments show that imposing units equivariance increases the generalization performance significantly, especially in out-of-distribution settings.

Figure 3 provides an illustration of the predicted orbits by the dimensional and the dimensionless methods in Experiment 1 and Experiment 2.

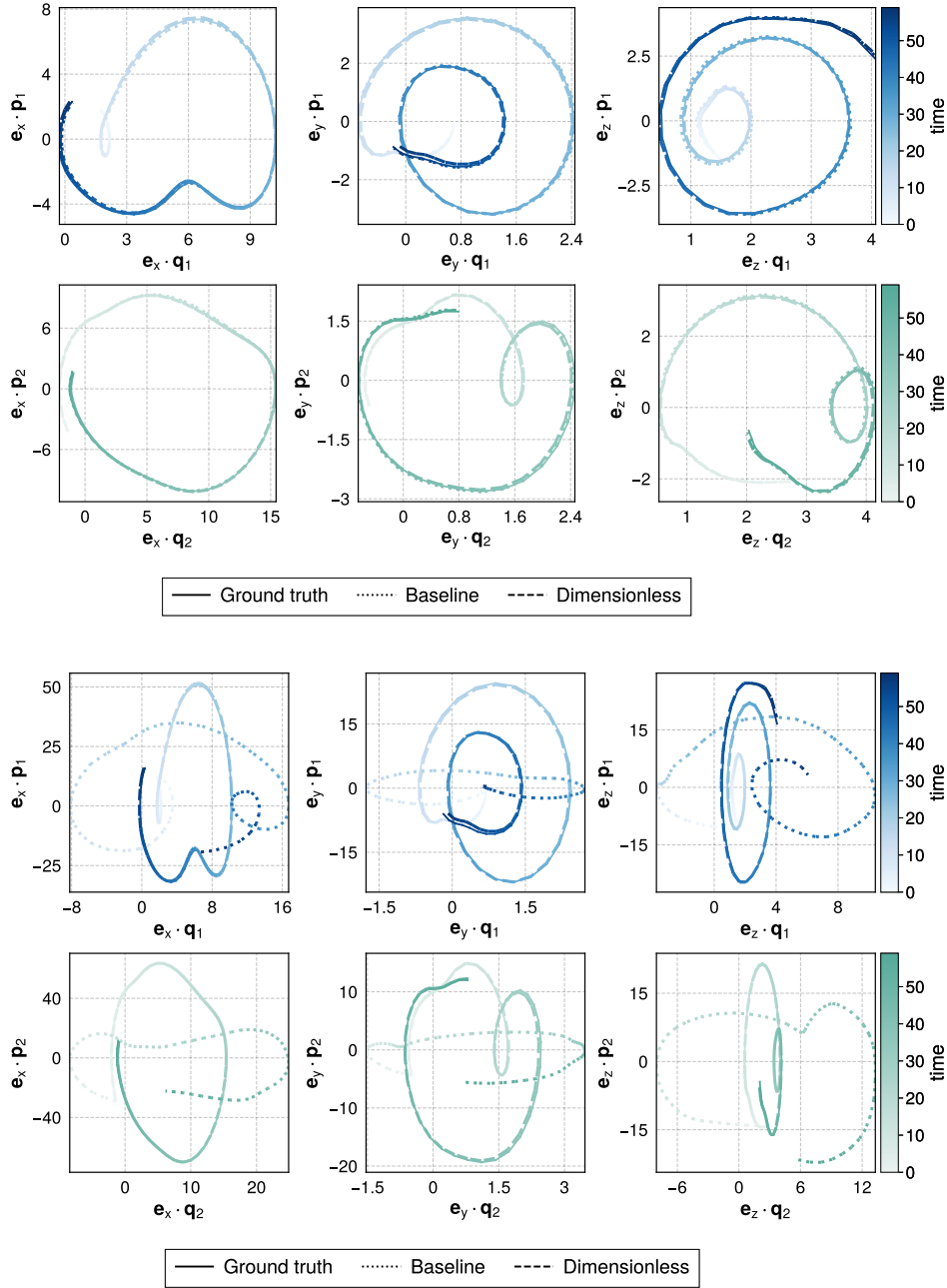


Figure 3: Ground truth and predictions of mass 1 (top) and 2 (bottom) in the phase space w.r.t. each dimension. **Top 6 panels:** Results from Experiment 1, where the test data are generated from the same distribution as those used for training. Here the dimensional scalar based MLPs exhibit slightly more accurate predictions for longer time scales. **Bottom 6 panels:** Results from Experiment 2, where we use the same test data in Experiment 1 but each with its inputs that have units of kg randomly scaled by a factor generated from $\text{Unif}(3, 7)$. Here the dimensionless scalar based MLP is able to provide comparable performance to Experiment 1, while using the dimensional scalars gives much worse predictions.

	description	default	units	
R	rainfall	0.375	$\ell \text{ d}^{-1} \text{ m}^{-2}$	
α	infiltration rate	0.2	d^{-1}	Dimensionless features
k_2	saturation const.	5	g m^{-2}	
W_0	water infiltration const.	0.1	—	
D_u	surface water diffusion	100	$\text{d}^{-1} \text{ m}^2$	
g_m	water uptake	0.05	$\ell \text{ g}^{-1} \text{ d}^{-1}$	
k_1	water uptake constant	5	$\ell \text{ m}^{-2}$	
δ_w	soil water loss	0.2	d^{-1}	
D_w	soil water diffusion	0.1	$\text{d}^{-1} \text{ m}^2$	
c	water to biomass	20	$\ell^{-1} \text{ g}$	
δ_v	vegetation loss	0.25	d^{-1}	
D_v	vegetation diffusion	0.1	$\text{d}^{-1} \text{ m}^2$	
T	total integration time	200	d	
δt	integration time step	0.005	d	
L	integration patch length	200	m	
δl	spatial step size	2	m	

Table 2: (Right) Parameters in the Rietkerk model and their units (Rietkerk et al., 2002). The bottom four parameters are parameters of the integration. (Left) Basis of dimensionless features found by our method.

Emulation: Arid vegetation model We further explore unit equivariance informed learning inspired by a non-linear problem in ecology⁴. In semi-arid environments, banded vegetation is a characteristic feature of plant self-organization which is modulated by the quantity of water available (Dagbovie and Sherratt, 2014). Inverting emergent vegetation patterns as a function of environmental changes is a central problem in ecology. Towards this end, a popular approach is the Rietkerk model, a set of differential equations relating surface water u , water absorbed into the soil w , and vegetation density v (Rietkerk et al., 2002).

The differential equations are

$$\begin{aligned}
 \frac{du}{dt} &= R - \alpha \frac{v + k_2 W_0}{v + k_2} u + D_u \nabla^2 u \\
 \frac{dw}{dt} &= \alpha \frac{v + k_2 W_0}{v + k_2} u - g_m \frac{v w}{k_1 + w} - \delta_w w + D_w \nabla^2 w \\
 \frac{dv}{dt} &= c g_m \frac{v w}{k_1 + w} - \delta_v v + D_v \nabla^2 v,
 \end{aligned} \tag{44}$$

where u, w, v are all functions of both two-dimensional spatial coordinates and time t , and the ∇^2 operator is the scalar second derivative operator (Laplacian) with respect to position. In detail, u denotes the surface water density (units of $\text{mm} = \ell \text{ m}^{-2}$), w is the soil water content (same units as u), and v is the vegetation density (units of g m^{-2}). Further, the time

4. See <https://dwh.gg/Rietkerk>.

derivative operator has units of d^{-1} , the Laplacian operator has units of m^{-2} , and the units of the other quantities (R , w_0 , g_m , and so on) can be inferred from the equations in (44). Here the natural base units are (ℓ , g , d , m). Note that as there is a conversion $1000 \ell = 1 m^3$, we could, in principle, reduce the base units by one. However, there is no direct communication between water volume and distance across the surface, so these units can be kept separate. In general, the units equivariance is more powerful when there are more independent base units, which leads to substantial design decisions for the investigator.

The Rietkerk model is determined by a set of dimensional parameters described in Table 2, and the initial conditions u_0, v_0, w_0 . We consider random initial conditions, and random choice of parameters, uniformly sampled between 0.5 and 1.5 times the default value. For each choice of parameters we use finite differences to estimate the derivatives and Laplacian, and integrate the Rietkerk model using Euler’s method with time step 0.005 d, in a $200 m \times 200 m$ grid, with 2 m pixel spacing.

We consider the task of predicting, from initial conditions, the average vegetation density after 200 d (which seems to coincide with the steady state solution of (44) at the default parameters). We produce a training set of 1000 points and a test set of 100. A significant portion of these simulations ended up on total vegetation death at finite time. We didn’t consider these examples for the regression task, extending our results to classification is a future direction.

We perform two forms of linear regression, a baseline regression and a unitless regression. The baseline regression uses 33 features: the dimensional parameters, their inverses, and the dimensionless constant 1 which describes affine linear functions. The dimensionless linear regression uses the method described in Section 4. It uses the Smith normal form to construct a basis of 12 dimensionless features, and it uses them, their inverses and the constant 1, obtaining 25 regression features. The results show that the dimensionless regression has significantly better performance in Figure 4.

We have only used this model as a toy here; we have merely explored the impact of dimensionally correct feature selection on average vegetation outcomes when data is generated from a well characterized ecological model. However, other interesting symbolic regression problems remains open. For example, is the Rietkerk model considered the most appropriate for modelling banded vegetation patterns in general? A recent approach has aimed to address the related inverse problem of determining the underlying structure of a nonlinear dynamical system from data (Brunton et al., 2016). In this approach, sparse regression and compressed sensing tools informed the selection of a small number of informative, non-linear terms hypothesized to impact an observed dynamics. Thus these kinds of problems present an intriguing venue for future exploration of units equivariance as a principled way to impose additional sparsity in a non-linear feature space which could further aid methods like that of Brunton et al. (2016) by restricting feature selection to units-equivariant, physically informative terms.

Symbolic regression: The black-body radiation law One of the most important moments in modern physics was the introduction of the quantum-mechanical constant h by Planck around 1900 (Planck, 1901). In our language, this discovery can be seen as a symbolic regression, in which Planck discovered a simple symbolic expression that accurately summarized a host of data sets on radiating bodies at different temperatures. The

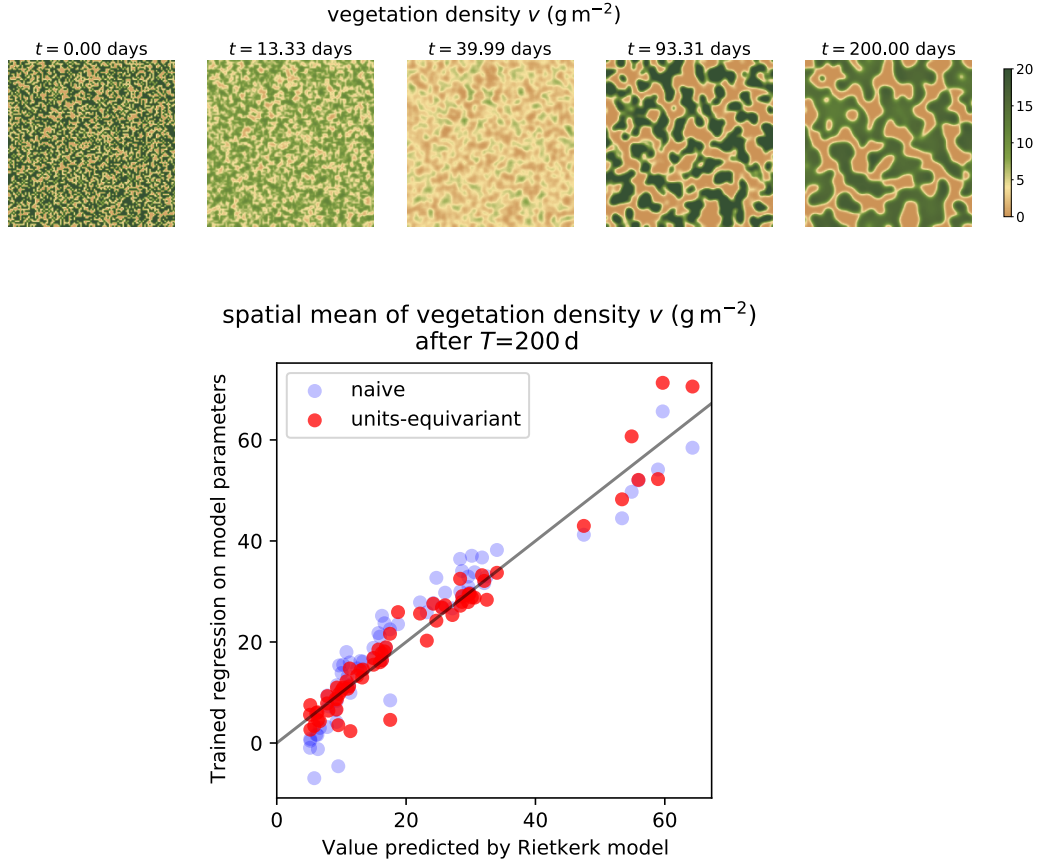


Figure 4: (Top) The evolution of vegetation density from random initialization according to a Rietkerk model. The model’s parameters are given in Table 2. (Bottom) We consider 1000 random initializations and evolutions according to random parameters sampled from a uniform distributions supported in $[0.5x, 1.5x]$ where x are the baseline Rietkerk parameters from Table 2 (the integration parameters remain fixed). Our regression task is to predict the spatial mean vegetation after 200 days as a function of the Rietkerk parameters. The light blue dots show the (naive) regression vs Rietkerk model for a linear regression on the model parameters, its inverses and the constant 1 (33 features in total) on a held out test set. The dark red dots correspond to a linear regression using a basis of dimensionless features obtained with our (units-equivariant) method, their inverses and the constant 1 (25 features in total) in the same test set. The naive regression has a test MSE of $26.3 \text{ g}^2 \text{ m}^{-4}$ whereas the units-equivariant regression has a MSE of $12.6 \text{ g}^2 \text{ m}^{-4}$. The Pearson correlation of the prediction and the target value is 0.94 for the naive regression and 0.97 for the units-equivariant regression.

	<i>description</i>	<i>units</i>	<i>comment</i>
$B_\lambda(\lambda; T)$	intensity	$\text{kg m}^{-1} \text{s}^{-3}$	regression label
λ	wavelength	m	variable feature
T	temperature	K	variable feature
c	speed of light	m s^{-1}	fundamental constant
k_B	Boltzmann's constant	$\text{kg m}^2 \text{s}^{-2} \text{K}^{-1}$	fundamental constant

Table 3: Labels and features in Planck's black-body radiation problem and their units.

dimensional constant h was introduced to explain the short-wavelength part of the radiation law, but it ended up being the governing constant for all quantum phenomena; it led to a simple prediction of the spectrum of the Hydrogen atom (Bohr, 1913) and is the core of the Schrödinger equation (Schrödinger, 1926); this was important!

The black-body radiation $B_\lambda(\lambda; T)$ from a perfectly radiating and absorbing (black) thermal source at temperature T is properly measured in intensity units, which are (or can be) energy per time per wavelength per area per solid angle. Because solid angles are dimensionless, this translates to SI units of $\text{J m}^{-3} \text{s}^{-1}$. The problem Planck faced was a set of measurements (labels) $B_\lambda(\lambda; T)$ at many wavelengths λ for bodies at multiple temperatures T . The input features λ, T, c, k_B and output labels $B_\lambda(\lambda; T)$ of the problem are summarized in Table 3, along with their units in the SI base unit system of kg, m, s, K.

In terms of the language illustrated in Figure 1, the decoder $g_{\mathbf{x}, \mathbf{v}}$ involves multiplying the dimensionless output of a dimensionless regression by a dimensional quantity with the same units as the labels $B_\lambda(\lambda; T)$. The only possible dimensional quantity that can be made out of the features that matches the dimensions of the labels is

$$\frac{c}{\lambda^4} k_B T, \quad (45)$$

which has units of intensity. The featurizer ϕ makes all possible dimensionless quantities out of the inputs. But wait, there are no (non-trivial) dimensionless features possible! In a dimensionless regression, the *only* available input feature is the dimensionless constant *unity*. That is, in our approach, the only possible outcome of the regression in this case is

$$B_\lambda(\lambda; T) = C \frac{c}{\lambda^4} k_B T, \quad (46)$$

where C is a universal constant. This is a classical dimensional-analysis argument or result! And it was probably one of the cases that inspired the original formulation of the Buckingham pi theorem (Buckingham 1914; although we emphasize that we are not making any historical claim).

There are two comments to make here. The first is that this form (46) is not a good fit to the data! Thus the method we are proposing here fails. The explanation for this failure is that there is a dimensionless constant, h (now known as Planck's constant) that is missing from our formulation in Table 3. The second is that this form (46) is a perfect fit to the data *at long wavelengths*. That is, at long wavelengths, where quantum occupation numbers are high, the problem behaves classically, and the data are extremely well explained by (46),

with $C = 2$. This result (with $C = 2$) is called the Rayleigh—Jeans law. If the reader is interested in the history of physics, the Rayleigh—Jeans law is the lynchpin of the ultraviolet catastrophe, which is a paradox of classical statistical mechanics, resolved by quantization.

What Planck discovered or realized is that the data could only be explained with the introduction of a new dimensional universal constant. He had choices for the dimensions of this constant, but he set it to have dimensions of energy times time. Planck’s symbolic regression led to the complete expression

$$B_\lambda(\lambda; T) = \frac{2 h c^2}{\lambda^5} \frac{1}{\exp(\frac{h c}{\lambda k_B T}) - 1}, \quad (47)$$

which reduces to (46) with $C = 2$ in the limit $\lambda \rightarrow \infty$. This result required the introduction of the dimensional constant h . This constant (and the physics it implies) resolved the ultraviolet catastrophe, and began the establishment of quantum mechanics. In the approach advocated here, we have no way to learn or discover missing dimensional constants. That is a limitation of our approaches, and motivates future work.

8. Discussion

In the above, we defined units equivariance for machine learning, with a focus on regression and complex functions. A function obeying this equivariance obeys the exact scalings that are required by the rules of dimensional analysis. These scalings must be obeyed by any theory or function in use in the natural sciences.

We developed a simple framework for implementing units equivariance into regression problems. This framework puts burdens on the investigator—burdens of having consistent units for all inputs, and also a comprehensive list of dimensional constants—but is otherwise lightweight in terms of modifying existing regression methods. We did not consider the important problems of learning dimensions, or discovery of missing dimensionless inputs, but these are worthy extensions of what we looked at here.

We argued that imposing units equivariance must improve the bias and variance of regression methods, both because it incorporates correct information, and also because it reduces model capacity at fixed complexity, often by an enormous factor. The equivariance also enables out-of-sample generalization, because a test set that doesn’t overlap a training set in dimensional inputs will often significantly overlap in dimensionless combinations of those inputs. We illustrated these effects empirically with a few simple experiments.

Units equivariance applies to all functions in the natural sciences. It won’t be useful everywhere. In particular, it is most useful when there are many independent units at play, and the full panoply of physical constants is known. This is not true, say, for standard image-recognition tasks, for which all the inputs have the same units (intensity in image pixels) and the physical quantities (involved in the identification of pandas and kittens, say) are not known. It is also not true in natural-science problems where there might be unknown physical constants or physical laws at play. The discovery of physical laws is often the discovery of dimensional physical constants, as our black-body radiation law example problem (Section 7) illustrates.

However, we are very optimistic about the usefulness of units equivariance in problems of emulation and symbolic regression. In these settings, all symmetries are exact, and often

all inputs (including all fundamental constants) are known (and have known units). In particular, some of the cleanest physics problems might be in the area of the growth of structure in the Universe, where there are very few dimensioned quantities and the physics is dominated by one force (gravity). These problems are of great interest at the present day, and have attracted very promising work with machine learning methods (for example, He et al. 2019; Berger and Stein 2019; Kodi Ramanah et al. 2020; Tröster et al. 2019).

Acknowledgments: It is a pleasure to thank Timothy Carson (Google), Miles Cranmer (Princeton), Samory Kpotufe (Columbia), Sanjoy Mahajan (Olin College), Bernhard Schölkopf (MPI-IS), Kate Storey-Fisher (NYU), and Wenda Zhou (NYU and Flatiron Institute) for valuable discussions. SV was partially supported by ONR N00014-22-1-2126, the NSF–Simons Research Collaboration on the Mathematical and Scientific Foundations of Deep Learning (MoDL) (NSF DMS 2031985), and the TRIPODS Institute for the Foundations of Graph and Deep Learning at Johns Hopkins University.

References

- Abien Fred Agarap. Deep learning using rectified linear units (RELU). *arXiv:1803.08375*, 2018.
- Martin Arjovsky. *Out of distribution generalization in machine learning*. PhD thesis, New York University, 2020.
- Henry S Baird. Document image defect models. In *Structured Document Image Analysis*, pages 546–556. Springer, 1992.
- Joseph Bakarji, Jared Callahan, Steven L Brunton, and J Nathan Kutz. Dimensionally consistent learning with buckingham pi. *arXiv:2202.04643*, 2022.
- Grigory Isaakovich Barenblatt. *Scaling and transformation groups. Renormalization group*, page 161–180. Cambridge Texts in Applied Mathematics. Cambridge University Press, 1996. doi: 10.1017/CBO9781107050242.009.
- Simon Batzner, Albert Musaelian, Lixin Sun, Mario Geiger, Jonathan P Mailoa, Mordechai Kornbluth, Nicola Molinari, Tess E Smidt, and Boris Kozinsky. Se (3)-equivariant graph neural networks for data-efficient and accurate interatomic potentials. *arXiv:2101.03164*, 2021.
- Shai Ben-David, John Blitzer, Koby Crammer, Alex Kulesza, Fernando Pereira, and Jennifer Wortman Vaughan. A theory of learning from different domains. *Machine learning*, 79(1):151–175, 2010.
- Gregory Benton, Marc Finzi, Pavel Izmailov, and Andrew Gordon Wilson. Learning invariances in neural networks. *arXiv:2010.11882*, 2020.
- Philippe Berger and George Stein. A volumetric deep convolutional neural network for simulation of mock dark matter halo catalogues. *Monthly Notices of the Royal Astronomical Society*, 482(3):2861–2871, 2019.

- Alberto Bietti, Luca Venturi, and Joan Bruna. On the sample complexity of learning under geometric stability. *Advances in Neural Information Processing Systems*, 34, 2021.
- Niels Bohr. I. on the constitution of atoms and molecules. *The London, Edinburgh, and Dublin Philosophical Magazine and Journal of Science*, 26(151):1–25, 1913.
- Simone Brugiapaglia, M Liu, and Paul Tupper. Invariance, encodings, and generalization: learning identity effects with neural networks. *arXiv preprint arXiv:2101.08386*, 2021.
- Steven L Brunton, Joshua L Proctor, and J Nathan Kutz. Discovering governing equations from data by sparse identification of nonlinear dynamical systems. *Proceedings of the national academy of sciences*, 113(15):3932–3937, 2016.
- Edgar Buckingham. On physically similar systems; illustrations of the use of dimensional equations. *Physical Review*, 4(4):345–376, 1914.
- Jameson Cahill, Dustin G Mixon, and Hans Parshall. Lie PCA: Density estimation for symmetric manifolds. *arXiv:2008.04278*, 2020.
- Shuxiao Chen, Edgar Dobriban, and Jane Lee. A group-theoretic framework for data augmentation. *Advances in Neural Information Processing Systems*, 33:21321–21333, 2020a.
- Zhengdao Chen, Lisha Li, and Joan Bruna. Supervised community detection with line graph neural networks. *International Conference on Learning Representations*, 2019a.
- Zhengdao Chen, Soledad Villar, Lei Chen, and Joan Bruna. On the equivalence between graph isomorphism testing and function approximation with gnns. In *Advances in Neural Information Processing Systems*, pages 15894–15902, 2019b.
- Zhengdao Chen, Lei Chen, Soledad Villar, and Bruna Joan. Can graph neural networks count substructures? *Advances in neural information processing systems*, 2020b.
- Taco S. Cohen and Max Welling. Group equivariant convolutional networks. In *Proceedings of the 33rd International Conference on International Conference on Machine Learning*, volume 48, page 2990–2999, 2016.
- Taco S Cohen and Max Welling. Steerable cnns. In *International Conference on Learning Representations (ICLR)*, 2017.
- Taco S. Cohen, Mario Geiger, Jonas Koehler, and Max Welling. Spherical cnns, 2018.
- Paul G Constantine, Zachary del Rosario, and Gianluca Iaccarino. Data-driven dimensional analysis: Algorithms for unique and relevant dimensionless groups. *arXiv:1708.04303*, 2017.
- Miles Cranmer, Alvaro Sanchez Gonzalez, Peter Battaglia, Rui Xu, Kyle Cranmer, David Spergel, and Shirley Ho. Discovering symbolic models from deep learning with inductive biases. *Advances in Neural Information Processing Systems*, 33:17429–17442, 2020.

- Ekin D Cubuk, Barret Zoph, Dandelion Mane, Vijay Vasudevan, and Quoc V Le. Autoaugment: Learning augmentation policies from data. *arXiv:1805.09501*, 2018.
- Ekin D Cubuk, Barret Zoph, Jonathon Shlens, and Quoc V Le. Randaugment: Practical automated data augmentation with a reduced search space. In *Proceedings of the IEEE/CVF Conference on Computer Vision and Pattern Recognition Workshops*, pages 702–703, 2020.
- Ayawoa S Dagbovie and Jonathan A Sherratt. Pattern selection and hysteresis in the rietkerk model for banded vegetation in semi-arid environments. *Journal of The Royal Society Interface*, 11(99):20140465, 2014.
- Tri Dao, Albert Gu, Alexander Ratner, Virginia Smith, Chris De Sa, and Christopher Ré. A kernel theory of modern data augmentation. In *International Conference on Machine Learning*, pages 1528–1537. PMLR, 2019.
- Jayanta Dey, Ashwin De Silva, Will LeVine, Jong Shin, Haoyin Xu, Ali Geisa, Tiffany Chu, Leyla Isik, and Joshua T Vogelstein. Out-of-distribution detection using kernel density polytopes. *arXiv:2201.13001*, 2022.
- David K Duvenaud, Dougal Maclaurin, Jorge Iparraguirre, Rafael Bombarell, Timothy Hirzel, Alán Aspuru-Guzik, and Ryan P Adams. Convolutional networks on graphs for learning molecular fingerprints. In *Advances in neural information processing systems*, pages 2224–2232, 2015.
- Bryn Elesedy. Provably strict generalisation benefit for invariance in kernel methods. *arXiv:2106.02346*, 2021.
- Bryn Elesedy and Sheheryar Zaidi. Provably strict generalisation benefit for equivariant models. *arXiv:2102.10333*, 2021.
- Nikolaos Evangelou, Noah J Wichrowski, George A Kevrekidis, Felix Dietrich, Mahdi Kooshkbaghi, Sarah McFann, and Ioannis G Kevrekidis. On the parameter combinations that matter and on those that do not. *arXiv:2110.06717*, 2021.
- Marc Finzi, Max Welling, and Andrew Gordon Wilson. A practical method for constructing equivariant multilayer perceptrons for arbitrary matrix groups. *arXiv:2104.09459*, 2021.
- Federico Frisone and Andrea Misiti. Buckingham theorem application to machine learning algorithms: methodology and practical examples. Master’s thesis, Politecnico di Milano, 2019.
- Fabian Fuchs, Daniel Worrall, Volker Fischer, and Max Welling. Se (3)-transformers: 3d rotation equivariant attention networks. *Advances in Neural Information Processing Systems*, 33, 2020.
- Fernando Gama, Elvin Isufi, Geert Leus, and Alejandro Ribeiro. Graphs, convolutions, and neural networks: From graph filters to graph neural networks. *IEEE Signal Processing Magazine*, 37(6):128–138, 2020.

- Ali Geisa, Ronak Mehta, Hayden S Helm, Jayanta Dey, Eric Eaton, Jeffery Dick, Carey E Priebe, and Joshua T Vogelstein. Towards a theory of out-of-distribution learning. *arXiv:2109.14501*, 2021.
- Justin Gilmer, Samuel S Schoenholz, Patrick F Riley, Oriol Vinyals, and George E Dahl. Neural message passing for quantum chemistry. In *Proceedings of the 34th International Conference on Machine Learning-Volume 70*, pages 1263–1272. JMLR. org, 2017.
- Samuel Greydanus, Misko Dzamba, and Jason Yosinski. Hamiltonian neural networks. In H. Wallach, H. Larochelle, A. Beygelzimer, F. d'Alché-Buc, E. Fox, and R. Garnett, editors, *Advances in Neural Information Processing Systems*, volume 32, 2019.
- Ben Gripiaios, Ward Haddadin, and Christopher G Lester. Lorentz-and permutation-invariants of particles. *Journal of Physics A: Mathematical and Theoretical*, 54(15):155201, 2021.
- Ward Haddadin. Invariant polynomials and machine learning. *arXiv:2104.12733*, 2021.
- Steve Hanneke and Samory Kpotufe. On the value of target data in transfer learning. *Advances in Neural Information Processing Systems*, 32, 2019.
- Trevor Hastie, Andrea Montanari, Saharon Rosset, and Ryan J. Tibshirani. Surprises in high-dimensional ridgeless least squares interpolation. *arXiv:1903.08560*, 2019. doi:10.48550/ARXIV.1903.08560. URL <https://arxiv.org/abs/1903.08560>.
- Siyu He, Yin Li, Yu Feng, Shirley Ho, Siamak Ravanbakhsh, Wei Chen, and Barnabás Póczos. Learning to predict the cosmological structure formation. *Proceedings of the National Academy of Sciences*, 116(28):13825–13832, 2019.
- Evelyne Hubert and George Labahn. Rational invariants of scalings from Hermite normal forms. In *Proceedings of the 37th International Symposium on Symbolic and Algebraic Computation*, pages 219–226, 2012.
- Wengong Jin, Regina Barzilay, and Tommi Jaakkola. Composing molecules with multiple property constraints. *arXiv:2002.03244*, 2020.
- Bingyi Kang and Jiashi Feng. Transferable meta learning across domains. In *UAI*, pages 177–187, 2018.
- George Em Karniadakis, Ioannis G Kevrekidis, Lu Lu, Paris Perdikaris, Sifan Wang, and Liu Yang. Physics-informed machine learning. *Nature Reviews Physics*, 3(6):422–440, 2021.
- K Kashinath, M Mustafa, A Albert, JL Wu, C Jiang, S Esmailzadeh, K Azizzadenesheli, R Wang, A Chattopadhyay, A Singh, et al. Physics-informed machine learning: Case studies for weather and climate modelling. *Philosophical Transactions of the Royal Society A*, 379(2194):20200093, 2021.
- Doogesh Kodi Ramanah, Tom Charnock, Francisco Villaescusa-Navarro, and Benjamin D Wandelt. Super-resolution emulator of cosmological simulations using deep physical models. *Monthly Notices of the Royal Astronomical Society*, 495(4):4227–4236, 2020.

- Risi Kondor. N-body networks: a covariant hierarchical neural network architecture for learning atomic potentials. *arXiv:1803.01588*, 2018.
- Yann LeCun, Bernhard Boser, John S Denker, Donnie Henderson, Richard E Howard, Wayne Hubbard, and Lawrence D Jackel. Backpropagation applied to handwritten zip code recognition. *Neural computation*, 1(4):541–551, 1989.
- Da Li, Yongxin Yang, Yi-Zhe Song, and Timothy M Hospedales. Learning to generalize: Meta-learning for domain generalization. In *Thirty-Second AAAI Conference on Artificial Intelligence*, 2018.
- Weixin Liang and James Zou. Metashift: A dataset of datasets for evaluating contextual distribution shifts and training conflicts. *arXiv:2202.06523*, 2022.
- Yishay Mansour, Mehryar Mohri, and Afshin Rostamizadeh. Domain adaptation: Learning bounds and algorithms. *arXiv:0902.3430*, 2009.
- Haggai Maron, Heli Ben-Hamu, Nadav Shamir, and Yaron Lipman. Invariant and equivariant graph networks. In *International Conference on Learning Representations*, 2018.
- Song Mei, Theodor Misiakiewicz, and Andrea Montanari. Learning with invariances in random features and kernel models, 2021.
- Christopher Morris, Martin Ritzert, Matthias Fey, William L Hamilton, Jan Eric Lenssen, Gaurav Rattan, and Martin Grohe. Weisfeiler and leman go neural: Higher-order graph neural networks. *Association for the Advancement of Artificial Intelligence*, 2019.
- Max Planck. On the law of the energy distribution in the normal spectrum. *Ann. Phys*, 4 (553):1–11, 1901.
- Max Rietkerk, Maarten C Boerlijst, Frank van Langevelde, Reinier HilleRisLambers, Johan van de Koppel, Lalit Kumar, Herbert HT Prins, and André M de Roos. Self-organization of vegetation in arid ecosystems. *The American Naturalist*, 160(4):524–530, 2002.
- Stephan Rudolph et al. On the context of dimensional analysis in artificial intelligence. In *International Workshop on Similarity Methods*. Citeseer, 1998.
- Alvaro Sanchez-Gonzalez, Victor Bapst, Kyle Cranmer, and Peter Battaglia. Hamiltonian graph networks with ODE integrators, 2019.
- Erwin Schrödinger. An undulatory theory of the mechanics of atoms and molecules. *Physical review*, 28(6):1049, 1926.
- Ruoqi Shen, Sébastien Bubeck, and Suriya Gunasekar. Data augmentation as feature manipulation: A story of desert cows and grass cows. *arXiv:2203.01572*, 2022.
- Richard P. Stanley. Smith normal form in combinatorics. *Journal of Combinatorial Theory, Series A*, 144:476–495, 2016.

- Nathaniel Thomas, Tess Smidt, Steven Kearnes, Lusann Yang, Li Li, Kai Kohlhoff, and Patrick Riley. Tensor field networks: Rotation- and translation-equivariant neural networks for 3d point clouds. *arXiv:1802.08219*, 2018.
- Ambler Thompson and Barry N. Taylor. *Guide for the Use of the International System of Units (SI); Natl. Inst. Stand. Technol. Spec. Publ. 811, 2008 ed.* National Institute of Standards and Technology, 2008.
- Tilman Tröster, Cameron Ferguson, Joachim Harnois-Déraps, and Ian G McCarthy. Painting with baryons: Augmenting N-body simulations with gas using deep generative models. *Monthly Notices of the Royal Astronomical Society: Letters*, 487(1):L24–L29, 2019.
- Silviu-Marian Udrescu and Max Tegmark. AI Feynman: A physics-inspired method for symbolic regression. *Science Advances*, 6(16):eaay2631, 2020.
- David A Van Dyk and Xiao-Li Meng. The art of data augmentation. *Journal of Computational and Graphical Statistics*, 10(1):1–50, 2001.
- Soledad Villar, David W Hogg, Kate Storey-Fisher, Weichi Yao, and Ben Blum-Smith. Scalars are universal: Equivariant machine learning, structured like classical physics. In *Thirty-Fifth Conference on Neural Information Processing Systems*, 2021.
- Binghui Wang, Jinyuan Jia, Xiaoyu Cao, and Neil Zhenqiang Gong. Certified robustness of graph neural networks against adversarial structural perturbation. *arXiv:2008.10715*, 2020a.
- Rui Wang, Karthik Kashinath, Mustafa Mustafa, Adrian Albert, and Rose Yu. Towards physics-informed deep learning for turbulent flow prediction. In *Proceedings of the 26th ACM SIGKDD International Conference on Knowledge Discovery & Data Mining*, pages 1457–1466, 2020b.
- Rui Wang, Robin Walters, and Rose Yu. Incorporating symmetry into deep dynamics models for improved generalization. *arXiv:2002.03061*, 2020c.
- Maurice Weiler and Gabriele Cesa. General $e(2)$ -equivariant steerable cnns. In H. Wallach, H. Larochelle, A. Beygelzimer, F. d'Alché-Buc, E. Fox, and R. Garnett, editors, *Advances in Neural Information Processing Systems*, volume 32, 2019.
- Maurice Weiler, Mario Geiger, Max Welling, Wouter Boomsma, and Taco Cohen. 3d steerable cnns: Learning rotationally equivariant features in volumetric data, 2018.
- Sebastien C Wong, Adam Gatt, Victor Stamatescu, and Mark D McDonnell. Understanding data augmentation for classification: when to warp? In *2016 international conference on digital image computing: techniques and applications (DICTA)*, pages 1–6. IEEE, 2016.
- Keyulu Xu, Weihua Hu, Jure Leskovec, and Stefanie Jegelka. How powerful are graph neural networks? *arXiv:1810.00826*, 2018.
- Weichi Yao, Kate Storey-Fisher, David W Hogg, and Soledad Villar. A simple equivariant machine learning method for dynamics based on scalars. *arXiv:2110.03761*, 2021.

Rose Yu, Paris Perdikaris, and Anuj Karpatne. Physics-guided ai for large-scale spatiotemporal data. In *Proceedings of the 27th ACM SIGKDD Conference on Knowledge Discovery & Data Mining*, KDD '21, page 4088–4089, New York, NY, USA, 2021. Association for Computing Machinery. ISBN 9781450383325. doi: 10.1145/3447548.3470793. URL <https://doi.org/10.1145/3447548.3470793>.